Applied Energy 334 (2023) 120703

Contents lists available at ScienceDirect

Applied Energy

journal homepage: www.elsevier.com/locate/apenergy

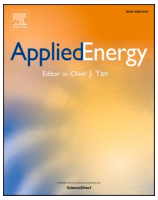

Integrated framework for modeling the interactions of plug-in hybrid electric vehicles aggregators, parking lots and distributed generation facilities in electricity markets

Mehdi Firouzi [a], Mehrdad Setayesh Nazar [a], Miadreza Shafie-khah [b], João P.S. Catalão [c,*]

[a] Shahid Beheshti University, Tehran, Iran
[b] School of Technology and Innovations, University of Vaasa, 65200 Vaasa, Finland
[c] Faculty of Engineering of the University of Porto (FEUP) and Research Center for Systems and Technologies (SYSTEC), 4200-465 Porto, Portugal

HIGHLIGHTS

- The proposed model presents an integrated modelling framework in day-ahead and real-time markets.
- The solution method compromises two-stage optimization processes for the optimization horizons.
- The impact of traffic in routes is modelled in the multi-stage multi-level optimization process.
- The sectionalizing process of the distribution system is modelled.

ARTICLE INFO

Keywords:
Active distribution network
Electric vehicles
Optimal scheduling
Aggregator
Parking lot

ABSTRACT

This paper presents an integrated framework for the optimal resilient scheduling of an active distribution system in the day-ahead and real-time markets considering aggregators, parking lots, distributed energy resources, and Plug-in Hybrid Electric Vehicles (PHEVs) interactions. The main contribution of this paper is that the impacts of traffic patterns on the available dispatchable active power of PHEVs in day-ahead and real-time markets are explored. A two stage framework is considered. Each stage consists of a four-level optimization procedure that optimizes the scheduling problems of PHEVs, parking lots and distributed energy resources, aggregators, and active distribution system. The distribution system procures ramp-up and ramp-down services for the upward electricity market in a real-time horizon. The active distribution system can utilize a switching procedure to sectionalize its system into a multi-microgrid system to mitigate the impacts of external shocks. The model was assessed by the 123-bus test system. The proposed algorithm reduced the interruption and operating costs of the 123-bus test system by about 94.56% for the worst-case external shock. Further, the traffic pattern decreased the available ramp-up and ramp-down of parking lots by about 58.61% concerning the no-traffic case.

1. Introduction

The Plug-in Hybrid Electric Vehicles (PHEVs) commitment strategies can change the operational planning of distribution systems in the normal and contingent conditions of the system [1]. The connected PHEVs (cPHEVs) can deliver active power and ancillary services to the Parking Lots (PLs) considering the forecasted day-ahead traffic patterns of routes; meanwhile, the PLs can procure energy and ancillary services for the energy aggregators. Further, the aggregator can transact energy and ancillary services with the Active Distribution System Operator (ADSO), Distributed Generation (DG) facilities, Smart Homes (SHs), Wind Turbines (WTs), PhotoVoltaic (PV) systems, Combined Heat and Power (CHP), and Energy Storage Systems (ESSs) [2].

As shown in Table 1, we can have: 1) PHEVs commitment strategies, and 2) combinations of the PHEVs and load commitment strategies.

Based on the above categorization and for the first group, Ref. [1] presents a multi-stage optimization process to assess the resiliency of the distribution system in the day-ahead and real-time horizons. The proposed algorithm considered the capacity withholding of energy resources in external shock conditions and evaluated the commitment of PHEVs in contingent conditions. Ref. [3] proposed an optimization

* Corresponding author.
E-mail address: catalao@fe.up.pt (J.P.S. Catalão).

https://doi.org/10.1016/j.apenergy.2023.120703
Received 18 July 2022; Received in revised form 10 November 2022; Accepted 14 January 2023
Available online 24 January 2023

Nomenclature

Abbreviation

ADSO	Active Distribution System Operator
ARIMA	Autoregressive Integrated Moving Average
CHP	Combined Heat and Power
CIC	Customer Interruption Cost
DA	Day-Ahead
DG	Distributed Generation
DLC	Direct Load Control
ESS	Electrical energy Storage System
EVEMS	Electrical Vehicle Energy Management System
MILP	Mixed Integer Linear Programming
MINLP	Mixed Integer Non Linear Programming
PL	Parking Lot
PHEV	Plug-in Hybrid Electrical Vehicle
cPHEVs	connected PHEVs
PV	Photovoltaic
RI	Resiliency Index
RT	Real-Time
SDERs	Static Distributed Energy Resources
SHs	Smart Homes
SOC	State of Charge
WT	Wind Turbine

Parameters

λ_{Fuel}	Fuel price
π_{ch}^{cPHEV}	Charge efficiency of cPHEV
π_{dch}^{cPHEV}	Discharge efficiency of cPHEV
T_p	Time duration of the scheduled interval
ΔU^{DG}	Ramp-up rate of distributed generation unit
cap^{ESS}	The capacity of energy storage
Γ	Robustness level parameter
$F_{ADSO\_LINE}^{Max}$	Max flow limit of ADSO feeder
W, W'	Weighting factors

Sets

ADSOS	Set of operating scenarios of the ADSO
AGGS	Set of operating scenarios of the aggregator
cPHEVS	Set of *cPHEV* operating state scenarios
Ω	Set of SDERs and parking lots
SDEROS	Set of operating states of SDERs and parking lots
ADSOEXS	The set of the operating scenario of the ADSO in external shock conditions
NBL	The set of boundary lines
NCU	Number of customers

Variables

$\alpha_{cPHEV}^{SR\_DA}$	cPHEV spinning reserve price
$\alpha_{cPHEV}^{AP\_DA}$	cPHEV active power price
$\alpha_{cPHEV}^{RR\_DA}$	cPHEV regulation reserve price
SR_{cPHEV}^{DA}	cPHEV spinning reserve
P_{cPHEV}^{DA}	cPHEV active power
RR_{cPHEV}^{DA}	cPHEV regulating reserve
ζ_{Fuel}	Fuel consumption of cPHEV
ϖ_{cPHEV}	Battery capacity of cPHEV
ΔSOC	Change in state of charge of cPHEV
$\alpha_{PL}^{AP\_DA}$	The price of electricity purchased from the parking lot
$\sum Penalty$	The penalties of mismatches of cPHEV day-ahead and real-time active power generations
γ^{ch}	Charge of cPHEV
γ^{dch}	Discharge of cPHEV
$t_{departure}$	cPHEV departure time
E_{desire}^{PHEV}	Desirable energy level of cPHEV
$\alpha_{\Omega}^{SR\_DA}$	SDERs and parking lots day-ahead spinning reserve price
$\alpha_{\Omega}^{AP\_DA}$	SDERs and parking lots day-ahead active power price
$\alpha_{\Omega}^{RP\_DA}$	SDERs and parking lots day-ahead reactive power price
$\alpha_{\Omega}^{RR\_DA}$	SDERs and parking lots day-ahead regulating reserve price
SR_{Ω}^{DA}	SDERs and PLs spinning reserve
P_{Ω}^{DA}	SDERs and PLs active power
Q_{Ω}^{DA}	SDERs and PLs reactive power
RR_{Ω}^{DA}	SDERs and PLs regulating reserve
C_{Ω}^{DA}	SDERs and PLs
I	Commitment of distributed generation unit
λ^{ch}	Charge of energy storage
λ^{dch}	Discharge of energy storage
P_t^{ESS}	The active power of energy storage
ΔP_{SH}^{DRP}	Load changes in the demand response process of the smart home
P^{PL}	Parking lot active power
$P^{PL\ Loss}$	Parking lot electrical loss
$P^{PL\ IMPORT}$	Parking lot imported active power
$\alpha_{AGG}^{SR\_DA}$	Aggregator day-ahead spinning reserve price
$\alpha_{AGG}^{AP\_DA}$	Aggregator day-ahead active power price
$\alpha_{AGG}^{RP\_DA}$	Aggregator day-ahead reactive power price
$\alpha_{AGG}^{RR\_DA}$	Aggregator day-ahead regulating reserve price
SR_{AGG}^{DA}	Aggregator spinning reserve
P_{AGG}^{DA}	Aggregator active power
Q_{AGG}^{DA}	Aggregator reactive power
RR_{AGG}^{DA}	Aggregator regulating reserve
C_{AGG}^{DA}	Operating cost of the aggregator
P^{Υ}	Active power of $\Upsilon \in AGG, PV, ESS, Load, CHP, DRP, WT, PL$
ΔP^{DLC}	Change in smart homes load that is carried out by direct load control process
$P_{Controllable}^{Load}$	Controllable loads of smart homes
$\alpha_{ADSO}^{SR\_DA}$	ADSO day-ahead spinning reserve price
$\alpha_{ADSO}^{AP\_DA}$	ADSO day-ahead active power price
$\alpha_{ADSO}^{RP\_DA}$	ADSO day-ahead reactive power price
$\alpha_{ADSO}^{RR\_DA}$	ADSO day-ahead regulating reserve price
SR_{ADSO}^{DA}	Day-ahead value of ADSO spinning reserve
P_{ADSO}^{DA}	Day-ahead value of ADSO active power
Q_{ADSO}^{DA}	Day-ahead value of ADSO reactive power
RR_{ADSO}^{DA}	Day-ahead value of ADSO regulating reserve
C_{ADSO}^{DA}	ADSO day-ahead operating cost
P_{ADSO}^{RT}	ADSO active power that is accepted by the upward market for the real-time market
P^{MTRANS}	The ADSO active power transaction with the upward market
P_{ADSO_LINE}	Active power of ADSO feeder
Q_{ADSO_LINE}	Reactive power of ADSO feeder
V	Voltage of ADSO bus
$C_{ADSO}^{Ext\_Shock\_DA}$	The ADSO operating cost in external shock conditions
X	Boundary line
$\beta_{cPHEV}^{AP\_RT}$	The submitted value of the cPHEV real-time market active power price
$\beta_{cPHEV}^{RAMP^+}$	The submitted value of the cPHEV real-time market ramp-up price
$\beta_{cPHEV}^{RAMP^-}$	The submitted value of the cPHEV real-time market ramp-down price
P_{cPHEV}^{RT}	cPHEV active power
$P_{cPHEV}^{RAMP^+}$	cPHEV ramp-up
$P_{cPHEV}^{RAMP^-}$	cPHEV ramp-down
c_{cPHEV}^{RT}	The cPHEV electricity generation cost
$c_{cPHEV}^{RAMP^-}$	The cPHEV ramp-down cost

$c_{cPHEV}^{RAMP^+}$	The cPHEV ramp-up cost
$\beta_{\Omega}^{AP\_RT}$	The submitted value of the SDERs and parking lots real-time active power price
$\beta_{\Omega}^{RP\_RT}$	The submitted value of the SDERs and parking lots real-time reactive power price
$\beta_{\Omega}^{RAMP^+}$	The submitted value of the SDERs and parking lots real-time ramp-up price
$\beta_{\Omega}^{RAMP^-}$	The submitted value of the SDERs and parking lots real-time ramp-down price
$P_{\Omega}^{RAMP^+}$	The accepted values of SDERs and PLs ramp-up
$P_{\Omega}^{RAMP^-}$	The accepted values of SDERs and PLs ramp-down
c_{Ω}^{RT}	The SDERs and PLs electricity generation cost
$c_{\Omega}^{RAMP^-}$	The SDERs and PLs ramp-down cost
$c_{\Omega}^{RAMP^+}$	The SDERs and PLs ramp-up cost
$\beta_{AGG}^{AP\_RT}$	The submitted aggregator real-time market active power price
$\beta_{AGG}^{RP\_RT}$	The submitted aggregator real-time market reactive power price
$\beta_{AGG}^{RAMP^+}$	The submitted aggregator real-time market ramp-up price
$\beta_{AGG}^{RAMP^-}$	The submitted aggregator real-time market ramp-down price
$P_{AGG}^{RAMP^-}$	The accepted values of aggregator ramp-down
$P_{AGG}^{RAMP^+}$	The accepted values of aggregator ramp-up
c_{AGG}^{RT}	The aggregator electricity generation cost
$c_{AGG}^{RAMP^-}$	The aggregator ramp-down cost
$c_{AGG}^{RAMP^+}$	The aggregator ramp-up cost
$\beta_{ADSO}^{AP\_RT}$	The submitted value of ADSO active power price
$\beta_{ADSO}^{RP\_RT}$	The submitted value of ADSO reactive power price
$\beta_{ADSO}^{RAMP^+}$	The submitted value of ADSO ramp-up price
$\beta_{ADSO}^{RAMP^-}$	The submitted value of ADSO ramp-down price
$P_{ADSO}^{RT}, Q_{ADSO}^{RT}$	ADSO real-time market active power and reactive power
$P_{ADSO}^{RAMP^+}, P_{ADSO}^{RAMP^-}$	ADSO ramp-up and ramp-down active power
c_{ADSO}^{RT}	The ADSO electricity generation cost
c_{ADSO}^{RAMP+}	The ADSO real-time market ramp-up cost
$c_{ADSO}^{RAMP^-}$	The ADSO real-time market ramp-down cost
$C_{ADSO}^{Ext\_Shock\_RT}$	The operating cost of the ADSO in external shock condition

process that modeled the interactions between the system operator, distribution generation owner, intermittent electricity generations, and parking lot of PHEVs. The proposed model was solved by mixed integer programming solver of GAMS. Ref. [4] presented assessed the PHEV commitment process considering demand response procedures. The photovoltaic electricity generation and energy storage systems were modeled. The uncertainties of electricity generation, prices, loads, microgrids commitments, and system contingencies were modeled. The parallel genetic algorithm was utilized for the optimization process. The traffic pattern, the smart home commitment, and aggregators' optimal day-ahead and real-time scheduling were not modeled in Refs. [1,3,4]. Ref. [5] investigated the reliability of the system considering vehicle-to-home and vehicle-to-grid modes of operation. The reliability of the system in the external shock conditions was increased considering the vehicle-to-grid commitment. Ref. [6] proposed a two-stage stochastic process to increase the resiliency level of the system considering PHEVs' commitment. The simulation results showed that the PHEV commitments increased the resiliency of the system. Ref. [7] investigated the impacts of the commitment process of PHEVs on the resiliency of the system in external shock conditions. However, the aggregators' optimal day-ahead and real-time scheduling and smart home commitment were not formulated in Refs. [5–7].

Ref. [8] evaluated a three-layer optimization algorithm for getting the optimal equilibrium points of retailers, charging stations, and PHEVs in the day-ahead market. The objective function of the first layer, second layer, and third layer minimized the PHEV costs, maximized the revenue of charging stations, and maximized the profit of retailers, respectively. The optimization was carried out for real data from San Francisco. The optimization process reduced the PHEVs costs by about 17.6%. Ref. [9] introduced real-time energy management of electric buses that utilized a predictive control model and considered the state of charge and velocity profile. The genetic algorithm with dynamic programming optimized the problem to find the optimal management solutions. Ref. [10] presented a four-stage optimization model for frequency support of PHEVs. The first stage determined the regulation signal generation. The second-stage problem optimized the frequency regulation capacity of PHEVs. The third and fourth stages optimized the charging station and aggregators' problems, respectively. Ref. [11] carried out the simulation process of the PHEVs energy management considering driving conditions, in which dynamic programming was utilized to solve the energy management problem of electric vehicles considering the state of charge, driving patterns, and velocity of vehicles. The fuel cost was reduced by about 14.8% using the proposed method. Ref. [12] proposed a flexible ramp market model that considered parking lots and demand response as the resources of ramp service providers. The model utilized a two-stage stochastic optimization process to minimize operating costs. Ref. [13] introduced a deep reinforcement-learning algorithm to control the energy consumption of PHEVs. The proposed model considered the traffic information and number of the electric bus. The output results were compared with the deep deterministic policy gradients model. Ref. [14] assessed a bi-level algorithm to schedule parking lots. The upper-level and lower-level problems maximized the profit of the parking lot and aggregator, respectively. The model considered the distributed generation facilities and load retailers. The process utilized the mathematical program with equilibrium constraints to solve the model. Ref. [15] introduced a model that utilized predictive control to minimize the emission and fuel consumption of PHEVs. The fuzzy logic controller optimized the real-time control strategy and the membership functions of the controller were determined by a genetic algorithm. The driving cycles and traffic patterns were considered in the model. Ref. [16] carried out the optimization process of PHEV aggregators in the day-ahead energy and ancillary services market using a robust model. The uncertainty of price was considered. The model found the Nash equilibrium of aggregators bidding. Ref. [17] utilized a dynamic programming algorithm to minimize the energy costs of the system in the flexible ramp market. However, Refs. [8–17] did not consider the integrated framework for modeling interactions of aggregators, parking lots, DGs, smart homes, CHPs, and intermittent electricity generations in the day-ahead and real-time energy and ancillary services markets. Further, Refs. [8–17] did not model the sectionalizing process of the distribution system to mitigate the impacts of external shocks.

Ref. [18] utilized a stochastic optimization algorithm to increase the resiliency of the system considering demand response programs and PHEVs commitment. Ref. [19] introduced an algorithm that maximized the resiliency of the system. The model considered the uncertainties of energy hubs, intermittent electricity generations, PHEVs, and demand response programs. Ref. [20] assessed a model for energy management of building microgrids in the day-ahead and real-time markets. Ref. [21] introduced an optimization process to increase the resiliency of the system that utilized emergency demand response considering the aging of facilities and reliability of the system. However, Refs. [18–21] did not model the interactions of aggregators, parking lots, DGs, smart homes,

Table 1
Comparison of the proposed method with other papers.

References		1	3	4	5	6	7	8	9	10	11	12	13	14	15	16	17	18	19	20	21	22	23	24	25	26	27	28	29	30	31	32	33	34	35	36	37	38	Proposed
Integrated Model of ADSO,		×	×	×	×	×	×	×	×	×	×	×	×	×	×	×	×	×	×	×	×	×	×	×	×	×	×	×	×	×	×	×	×	×	×	×	×	×	✓
Switching of system in ext. shock		✓	×	×	×	×	×	×	×	×	×	×	×	×	×	×	×	×	×	×	×	✓	×	✓	×	✓	✓	×	✓	✓	×	×	×	×	×	×	×	×	×	✓
Commitment of smart homes		×	×	×	×	×	×	×	×	×	×	×	×	×	×	×	×	×	×	×	×	×	×	×	×	×	×	×	×	×	×	×	×	×	×	×	×	×	✓
Considering traffic pattern		×	×	×	×	×	×	×	×	×	✓	×	✓	×	✓	×	×	×	×	×	×	×	×	×	×	×	×	×	×	×	×	×	×	×	×	×	✓	✓	✓
Real-time pricing		×	×	✓	×	✓	×	×	×	✓	×	×	×	×	×	×	×	✓	×	×	×	×	×	×	×	×	×	×	×	×	×	×	×	×	×	×	×	×	✓
Ancillary Services of PLs		×	×	×	×	×	×	×	×	✓	×	×	×	×	×	✓	×	×	×	×	×	×	×	×	×	×	×	×	×	×	×	×	×	×	×	×	×	×	✓
Resiliency Index		✓	×	×	×	×	×	×	×	×	×	×	×	×	×	×	×	×	×	×	×	×	×	×	×	×	×	×	×	✓	✓	×	×	×	✓	×	×	×	×	✓
Ramp Market		×	×	×	×	×	×	×	×	×	×	✓	×	×	×	×	✓	×	×	×	×	×	×	×	×	×	×	×	×	×	×	×	×	×	×	×	×	×	×	✓
Method	MILP	×	×	×	×	✓	×	×	×	×	×	✓	×	✓	×	×	×	✓	✓	✓	×	✓	×	×	×	×	×	×	×	×	×	✓	×	×	×	✓	×	×	×	×
	MINLP	×	×	×	×	×	×	×	×	×	×	×	×	×	×	×	×	×	×	×	×	×	×	✓	✓	×	×	×	×	×	×	×	×	×	×	✓	×	×	×	×
	Heuristic	✓	✓	✓	✓	×	✓	✓	✓	✓	✓	×	✓	×	✓	✓	✓	×	×	×	✓	×	✓	×	×	✓	✓	✓	✓	✓	×	✓	✓	✓	×	×	✓	✓	✓
Model	Determ.	×	✓	✓	✓	×	✓	×	✓	✓	×	×	✓	×	×	✓	×	×	×	×	✓	✓	✓	×	✓	✓	✓	✓	×	✓	×	×	×	×	×	×	✓	✓	×
	Stoch.	✓	×	×	×	✓	×	✓	×	×	×	✓	×	✓	✓	×	×	✓	✓	✓	×	×	×	✓	×	×	×	×	✓	×	✓	✓	✓	✓	✓	✓	×	×	✓
Objective Function	ADSO Benefit	×	×	×	×	×	×	×	×	×	×	×	×	×	×	×	×	✓	×	✓	✓	×	×	×	×	×	×	×	✓	×	✓	×	×	×	×	✓	✓	✓	✓
	Gen. Cost	✓	✓	✓	×	✓	×	✓	×	✓	×	✓	×	✓	×	×	×	✓	✓	✓	✓	✓	✓	✓	✓	×	✓	✓	✓	✓	✓	✓	✓	✓	✓	✓	×	×	✓
	Agg. Benefit	×	×	×	×	×	×	✓	×	✓	×	✓	×	✓	×	✓	×	×	×	×	×	×	×	×	×	×	×	×	×	×	✓	×	×	×	×	✓	×	×	✓
	SHs Benefit	×	×	×	×	×	×	×	×	×	×	×	×	×	×	×	×	×	×	×	×	×	×	×	×	×	×	×	×	×	×	×	×	×	×	×	×	×	✓
	PLs Benefit	×	×	×	×	×	×	✓	×	✓	✓	✓	×	✓	×	×	×	×	×	×	×	×	×	×	×	×	×	×	×	×	✓	×	×	×	✓	✓	×	×	✓
	Storage Cost	✓	✓	✓	×	✓	×	×	×	×	×	✓	×	×	×	×	×	✓	✓	✓	✓	×	×	×	×	✓	×	×	×	✓	×	×	×	✓	✓	×	×	✓
	Secu. Costs	✓	×	×	✓	×	×	×	×	×	×	×	×	×	×	×	×	✓	×	✓	×	×	✓	✓	✓	×	×	✓	×	✓	✓	×	×	×	✓	✓	×	×	✓
	PHEV cost	✓	✓	×	✓	✓	✓	✓	✓	✓	×	✓	✓	✓	✓	✓	✓	✓	✓	✓	×	×	×	×	×	×	×	×	×	×	✓	×	×	×	✓	✓	✓	✓	✓
	WT	✓	✓	×	×	✓	×	×	×	×	×	✓	×	×	×	×	×	×	×	✓	✓	×	×	×	×	×	×	×	×	✓	×	✓	×	×	✓	✓	✓	×	×	✓
	PV	✓	✓	✓	×	✓	×	×	×	×	×	✓	×	×	×	×	×	×	×	×	✓	×	×	×	×	×	×	×	×	✓	×	✓	×	×	✓	✓	✓	×	×	✓
DA-Market		✓	✓	✓	✓	×	✓	✓	×	×	×	✓	×	✓	×	✓	×	✓	✓	✓	✓	✓	✓	✓	✓	×	✓	✓	×	✓	×	✓	✓	✓	✓	✓	✓	×	✓	✓
RT- Market scheduling		✓	×	×	×	✓	×	×	×	×	×	✓	×	×	×	×	✓	×	×	✓	×	×	×	×	×	×	×	×	×	×	✓	×	×	×	×	✓	✓	×	✓
Uncertainty Model	PHEV Energy Consumption	×	×	×	×	×	×	×	×	×	×	✓	×	✓	✓	×	×	×	×	×	×	×	×	×	×	×	×	×	×	×	×	×	×	×	×	×	×	×	✓
	SHs DRP	×	×	×	×	×	×	×	×	×	×	×	×	×	×	×	×	✓	✓	✓	×	×	×	×	×	×	×	×	×	×	×	×	×	×	×	×	×	×	✓
	Traffic Pattern	×	×	×	×	×	×	×	×	×	×	×	×	×	✓	×	×	×	×	×	×	×	×	×	×	×	×	×	×	×	×	×	×	×	×	×	×	×	✓
	ADSO Acc. DA Market	×	×	×	×	×	×	×	×	×	×	×	×	×	×	×	×	×	×	×	×	×	×	×	×	×	×	×	×	×	×	×	×	×	×	×	×	×	✓
	ADSO Acc. RT Market	×	×	×	×	×	×	×	×	×	×	×	×	×	×	×	×	×	×	×	×	×	×	×	×	×	×	×	×	×	×	×	×	×	×	×	×	×	✓
	SDERs and PLs Acc.	×	×	×	×	×	×	×	×	×	×	×	×	×	×	×	×	×	×	×	×	×	×	×	×	×	×	×	×	×	×	×	×	×	×	×	×	×	✓
	External Shock	✓	×	×	×	×	×	×	×	×	×	×	×	×	×	×	×	×	×	×	✓	×	×	×	×	×	×	×	×	×	✓	×	✓	×	✓	✓	×	×	✓
	Loads	✓	×	×	×	×	×	×	×	×	×	✓	×	×	×	×	×	×	×	✓	×	×	×	×	×	×	×	×	×	✓	×	✓	×	×	×	✓	✓	×	×	✓
	Inter. electricity	✓	×	✓	×	✓	×	×	×	×	×	✓	×	×	×	×	×	×	×	×	×	×	×	×	×	×	×	×	×	✓	×	✓	×	✓	×	✓	✓	×	×	✓

CHPs, and intermittent electricity generations in the markets.

Other papers did not consider the PHEV commitment process in the resiliency assessment and only optimized the operational scheduling of the distribution system in the external shock conditions considering the switching process of normally opened/closed switches. Ref. [22] introduced an energy management model to schedule the networked microgrids and reduce the impact of external shocks. The shed load was reduced by about 57.3% by utilizing the demand response process. Ref. [23] utilized a three-stage optimization process. In the first stage and second stages, the hardening process of the system and the switching process of the system were carried out, respectively. Ref. [24] assessed a sectionalizing process to increase the resiliency of the system. The optimal scheduling of the distributed energy resources was carried out. Ref. [25] performed the simulation process for microgrid. The model utilized iterative linear programming and the case studies were performed for the 69-bus PG&E and 33-bus IEEE systems. Ref. [26] introduced a two-stage algorithm for optimal scheduling of microgrids and distribution system. Ref. [27] utilized graph theory to schedule the distribution system and increase the resiliency level of the system. Ref. [28] clustered the distribution system into multi-microgrids in external shock conditions. The Pareto optimality method determined the values of energy not supplied, energy loss, reactive power not supplied, and voltage deviations. Ref. [29] scheduled the networked microgrids considering a resiliency index. The uncertainties of intermittent electricity generations and market prices were modeled. The shed load was reduced by about 78.36% concerning the base case. Ref. [30] introduced an optimization approach for the resilient scheduling of networked microgrids. The model determined the proposed resiliency index using the analytical hierarchical algorithm. Refs. [22–30] did not model the aggregators, parking lots, DGs, smart homes, CHPs, and intermittent electricity generations in the day-ahead and real-time energy and ancillary services markets. Further, the traffic pattern on the route was not modeled in Ref. [22–30].

Ref. [31] proposed an algorithm for the optimal scheduling of active distribution networks. Ref. [31] did not reflect the resilient operation of the distribution system. Further, Ref. [31] did not evaluate the smart homes' categorization. Ref. [32] introduced a framework for stochastic optimization of the resilient distribution system that utilizes a dynamic

microgrid formation process. The model considered the droop control and frequency regulation processes. Ref. [33] assessed the impacts of the electric vehicle-oriented incentive mechanism to increase the resiliency of the distribution system. The restoration process and incentive mechanism of electric vehicles were optimized using the robust optimization process and Nash game theory, respectively. Ref. [34] optimized the simultaneous utilization of automated switches and distributed energy resources. Ref. [35] introduced a stochastic optimization process to increase the resiliency of networked microgrids considering intermittent power generations, electric vehicles, and energy storage. The non-linear model was solved using linearization techniques. The minimization of costs and maximization of renewable generations were considered. Ref. [36] assessed a multi-carrier system using a risk-averse strategy. The model utilized pre-event preventive and post-event corrective strategies to increase the resiliency of the multi-carrier system. The algorithm determined the optimal value of the risk-control parameter. Refs. [31–36] did not model the commitments of aggregators, parking lots, DGs, smart homes, CHPs, and intermittent electricity generations in the ancillary services markets. Further, the traffic patterns on the routes, the smart homes categorization, contribution modes, and their commitments were not modeled [31–36].

Ref. [37] proposed the optimal charge scheduling and electric vehicle routing processes considering the traffic networks and electrical system interactions. The model scheduled the electric vehicle charging process, and then, the electrical system and traffic networks status data were updated and the electric vehicles operating conditions were determined. The combined generalized benders decomposition algorithm and distributed biased min consensus method were utilized to solve the problems. Ref. [38] introduced an optimal charging scheduling procedure considering the electric vehicles' transportation system data and vehicles' velocity. The electrical system data such as voltage offset rate, voltage qualification rate, power loss of the network, the standard deviation of the load, and margin of the power supply capacity were considered in the optimization model. The simulation results revealed that the proposed model improved the efficiency of the transportation system and electrical operating variables. Refs. [37–38] did not model the commitments of smart homes in the ancillary services markets and the switching of the electrical distribution system.

As shown in Table 1, an integrated framework for modeling the interactions of plug-in hybrid electric vehicles' aggregators, parking lots, distributed generation facilities, and smart homes contribution scenarios in ancillary service markets is less common in the literature. In this paper, a framework for optimal day-ahead and real-time scheduling of distribution system, aggregators, distributed energy facilities, and smart homes is proposed.

Based on the above categorization and the detailed descriptions of recent papers, the contributions of this paper are depicted in the following:

- The proposed model presents an integrated framework for modeling the interactions of aggregators, parking lots, DGs, smart homes, CHPs, and intermittent electricity generations in day-ahead and real-time energy and ancillary services markets.
- The solution method compromises two-stage optimization processes. Each stage consists of a four-level optimization procedure that optimizes the PHEVs, parking lots and distributed energy resources, aggregators, and active distribution system scheduling problems.
- The impact of traffic on routes is modeled in the multi-stage multi-level optimization process. In addition, the sectionalizing process of the distribution system to mitigate the impacts of external shocks considering the available dispatchable energy resources of PHEVs, parking lots, and aggregators is modeled.

2. Modeling and formulation of the problem

Fig. 1 presents the interface among various system elements.

ADSO transacts power, reserve, and ramp service with upward electricity market. Further, the aggregators transact power, reserve, and ramp service with the ADSO. Different aggregators are procuring energy and ancillary services for the ADSO. A smart home can participate in the demand response program and deliver active power to its aggregator. The aggregator purchases active power, spinning reserve, and regulation reserve from CHP units, parking lots, and fossil-fueled DGs.

It is assumed that the aggregator can only purchase active power

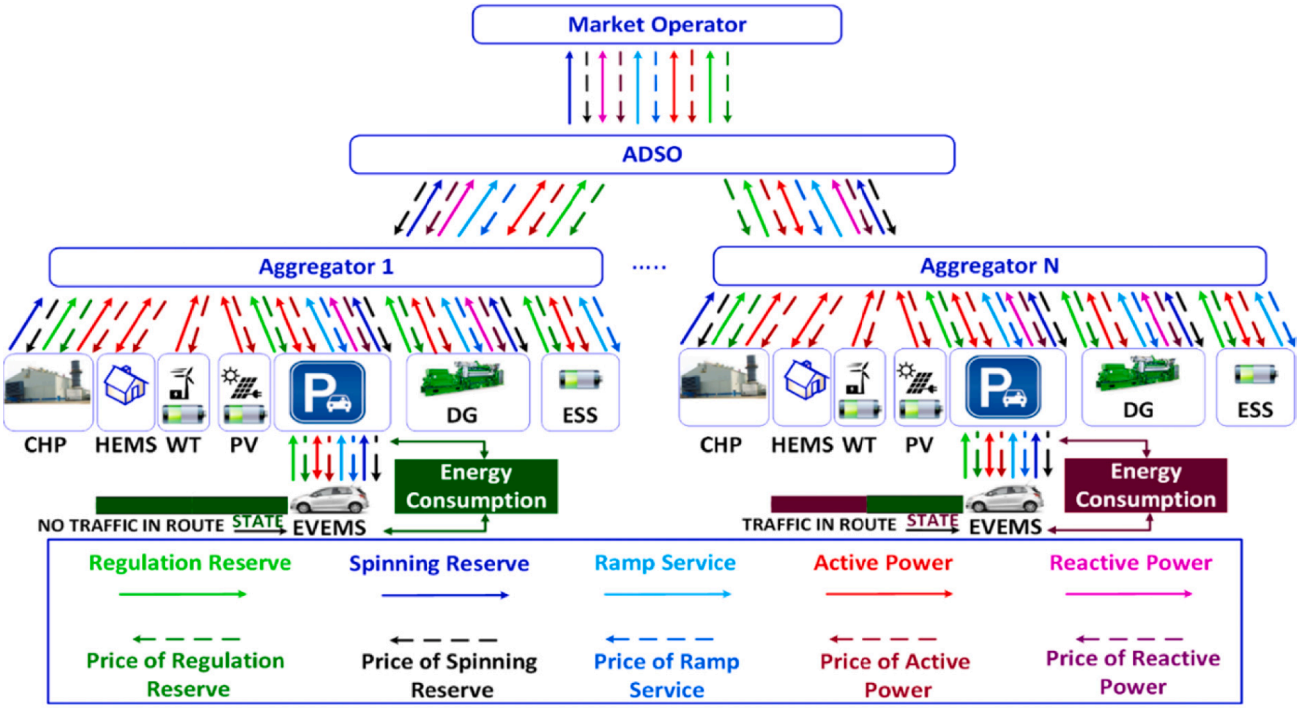

Fig. 1. Interface among various system elements.

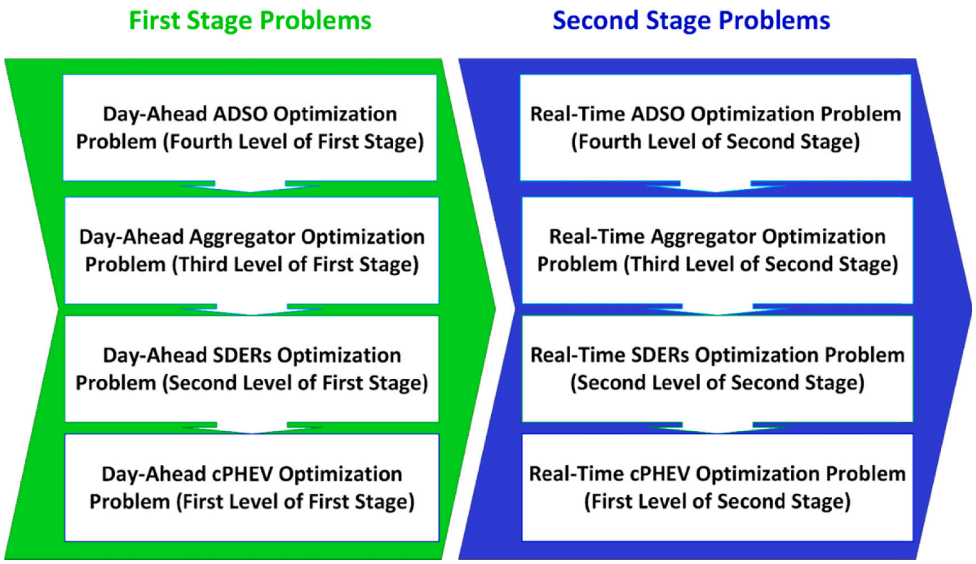

Fig. 2. The procedure of the proposed optimization algorithm.

from PV and WT systems based on the fact that these facilities are equipped with ESSs and the aggregator can dispatch their active power. Further, the connected PHEV is equipped with the Electrical Vehicle Energy Management System (EVEMS). The cPHEV can deliver ramping service to the parking lot in the real-time market. The traffic patterns are forecasted for the day-ahead horizon and are updated based on the real-time signal [13]. The EVEMS receives day-ahead and real-time traffic signals and estimates the energy consumption of cPHEV for a probable trip. Then, the cPHEV determines the optimal rates of active power transactions and delivers ramping ancillary services. Combined heat and power units, smart homes, storage facilities, wind turbines, photovoltaic systems, and distributed generation units are known as Static Distributed Energy Resources (SDERs).

The cPHEV, parking lots, and static distributed energy resources can participate in the day-ahead and real-time markets. Based on the described energy and ancillary service transactions, a two-stage process is suggested (Fig. 2).

The first levels of the optimization processes determine the optimal scheduling of the ADSO. The second level problems find the aggregators scheduling. The third level problems optimize the parking lots and static distributed energy resources scheduling problem. Finally, the fourth-level problems establish the cPHEVs scheduling.

The following uncertainties are pondered: 1) day-ahead cPHEVs energy consumptions and change in SOC based on the forecasted traffic patterns on routes that are dependent on the PHEV arrivals and departures; 2) vol./prices of cPHEVs; 3) vol./prices of parking lots and SDERs; 4) vol./prices of aggregators'; 5) day-ahead demand and intermittent generation; 6) demand response and external shocks.

The day-ahead cPHEV energy consumption and change in SOC are dependent on the PHEV arrivals and departures. Numerous scenarios should be generated for the PHEV arrival and departure for the day-ahead optimization process. Then, based on the PHEV arrival and departure scenarios, the scenarios of day-ahead cPHEVs energy consumptions and change in SOC based on the forecasted traffic patterns on routes were generated.

2.1. Day-Ahead optimization problems

2.1.1. The cPHEV Day-Ahead optimization objective function

The objective function is given as (1):

$$Max\ \mathbb{F}^{\mathrm{DA}}_{\mathrm{cPHEV}} = \sum_{\mathrm{cPHEVS}} \mathrm{prob}\cdot\left(\alpha^{\mathrm{SR\_DA}}_{\mathrm{cPHEV}}\cdot \mathrm{SR}^{\mathrm{DA}}_{\mathrm{cPHEV}} + \alpha^{\mathrm{AP\_DA}}_{\mathrm{cPHEV}}\cdot \mathrm{P}^{\mathrm{DA}}_{\mathrm{cPHEV}} + \alpha^{\mathrm{RR\_DA}}_{\mathrm{cPHEV}}\cdot \mathrm{RR}^{\mathrm{DA}}_{\mathrm{cPHEV}} - \zeta_{\mathrm{Fuel}}\cdot\lambda_{\mathrm{Fuel}} - \varpi_{cPHEV}\cdot\Delta SOC\cdot\alpha^{AP\_DA}_{PL} - \sum Penalty_{cPHEV}\right) \quad (1)$$

The $\zeta_{Fuel}, \lambda_{Fuel}, \varpi_{cPHEV}, \Delta SOC, \alpha^{AP\_DA}_{PL}$ are the fuel consumption of cPHEV, fuel price, battery capacity of cPHEV, change in State of Charge (SOC) of cPHEV, and the price of electricity purchased from the parking lot, respectively. The traffic patterns are forecasted for the day-ahead horizon [13]. The EVEMS receives day-ahead traffic signals and estimates the energy consumption (ζ_{Fuel}) and change in SOC of cPHEV (ΔSOC) for a probable trip. Further, the EVEMS determines the values of $\alpha^{SR\_DA}_{cPHEV}, \alpha^{AP\_DA}_{cPHEV}, \alpha^{RR\_DA}_{cPHEV}$ based on historical data [13,14]. Eq. (1) can be approximately maximized by the EVEMS considering the estimated values of P^{RT}_{cPHEV}, $SR^{DA}_{cPHEV}, P^{DA}_{cPHEV}, RR^{DA}_{cPHEV}$. Then, the parking lot optimization process should determine the values of P^{RT}_{cPHEV}, $SR^{DA}_{cPHEV}, P^{DA}_{cPHEV}$, RR^{DA}_{cPHEV} variables. Finally, the accepted values of $SR^{DA}_{cPHEV}, P^{DA}_{cPHEV}$, RR^{DA}_{cPHEV} variables are sent to PHEVs by the corresponding PLs and the value of Eq. (1) can be accurately maximized by the EVEMS.

The cPHEV day-ahead optimization objective function objective compromises the following terms: 1) the revenue of spinning reserve sold to the parking lot ($\alpha^{SR\_DA}_{cPHEV}\cdot SR^{DA}_{cPHEV}$); 2) revenue of active power offered to the parking lot ($\alpha^{AP\_DA}_{cPHEV}\cdot P^{DA}_{cPHEV}$); 3) the revenue of regulating reserve sold to the parking lot ($\alpha^{RR\_DA}_{cPHEV}\cdot RR^{DA}_{cPHEV}$); 4) the fuel cost of PHEV ($\zeta_{Fuel}\cdot\lambda_{Fuel}$); 5) the cost of PHEV battery commitment ($\varpi_{cPHEV}\cdot\Delta SOC\cdot\alpha^{AP\_DA}_{Agg}$); 6) and the penalties of mismatches of cPHEV day-ahead and real-time active power generations ($\sum Penalty_{cPHEV}$).

Eq. (1) is subjected to the following constraints:

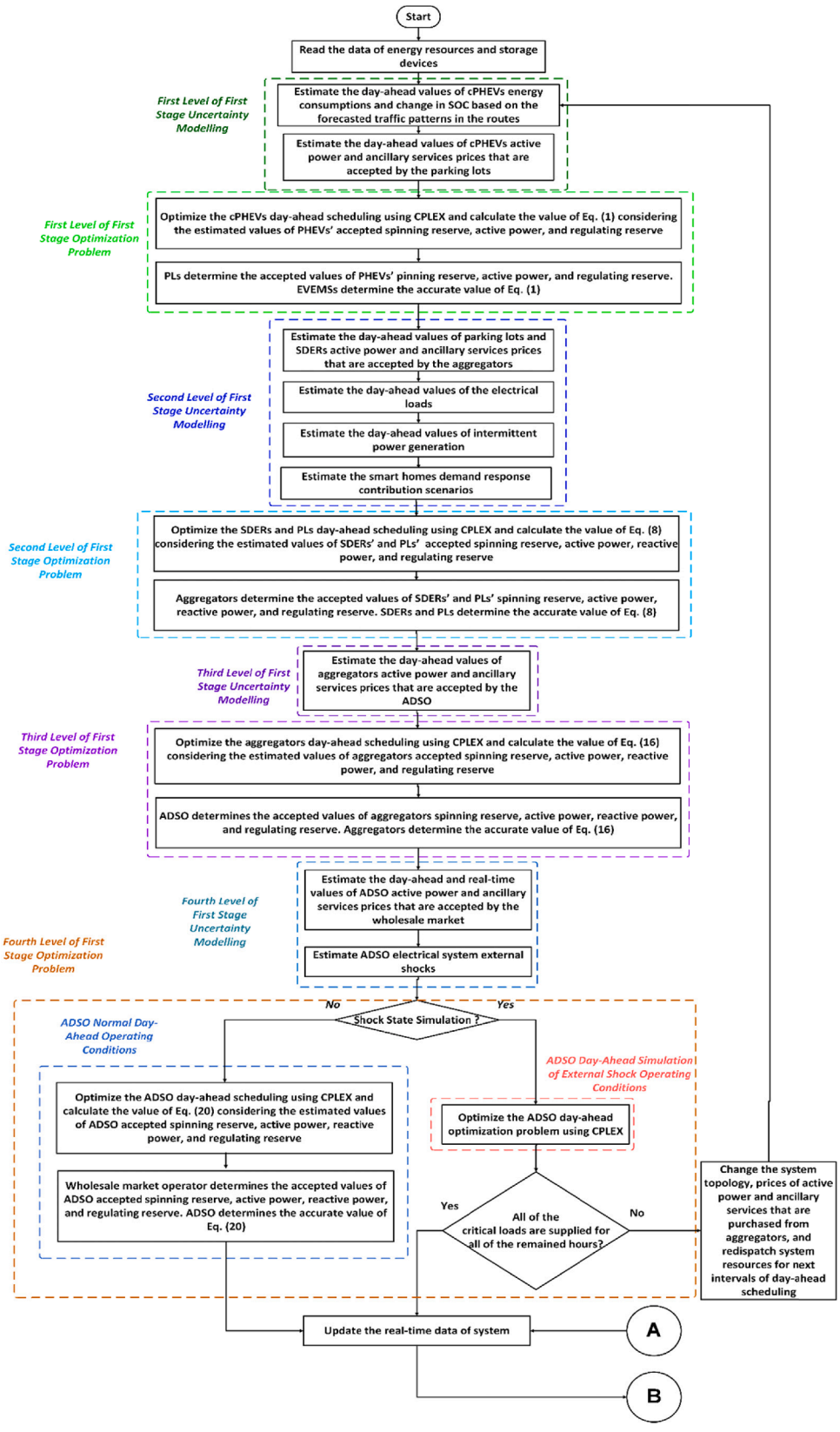

(a)

Fig. 3. (a) Day-ahead process, (b) Real-time process.

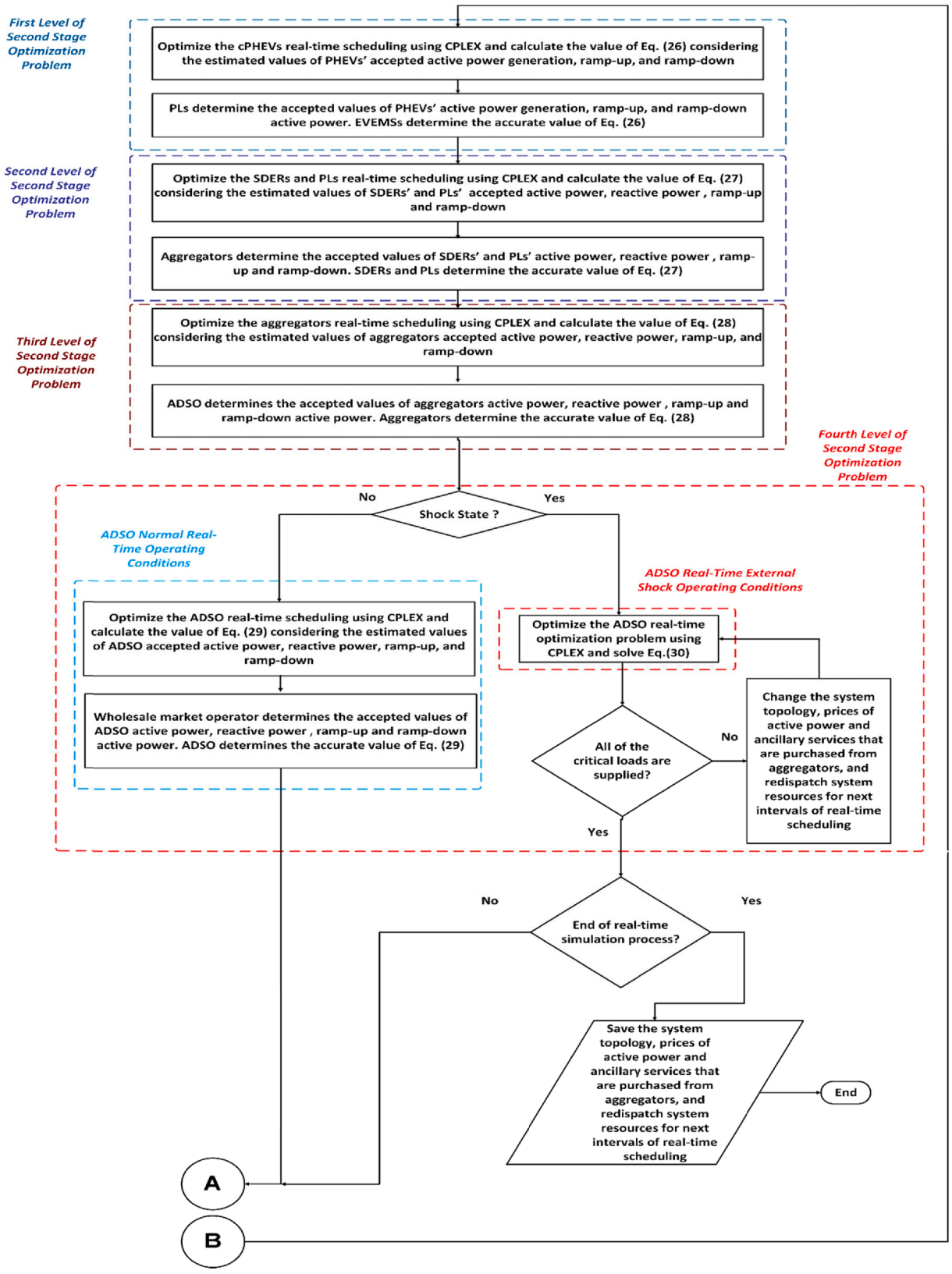

(b)

Fig. 3. (*continued*).

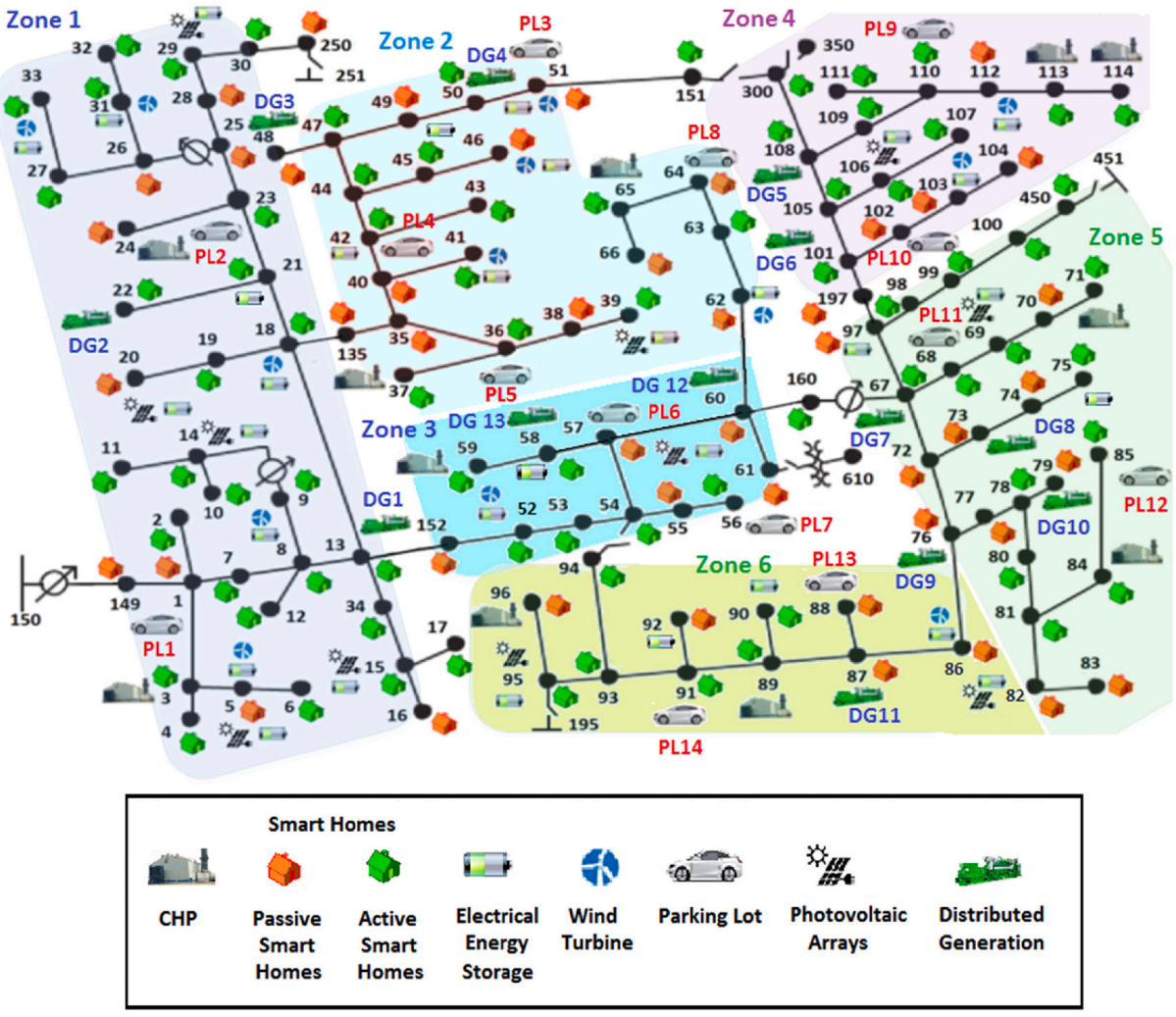

Fig. 4. 123-bus test system.

Table 2
The scenario generation and reduction scenarios for the 33-bus system.

System parameter	Value
No. of day-ahead cPHEVs energy consumptions and change in SOC based on the forecasted traffic patterns on routes scenarios	1000
No. of volumes/prices of day-ahead cPHEVs	1000
No. of volumes/prices of day-ahead parking lots and SDERs	1000
No. of volumes/prices of day-ahead aggregators	1000
No. of volumes/prices of day-ahead ADSO	1000
No. of demand response scenarios	1000
No. of day-ahead demands	1500
No. of day-ahead intermittent generation	1000
No. of ADSO external shocks	1000
No. of reduced scenarios of day-ahead cPHEVs energy consumptions and change in SOC based on the forecasted traffic patterns on routes scenarios	10
No. of the volumes/prices of red. scenarios of cPHEVs	10
No. of the volumes/prices of red. scenarios of parking lots and SDERs	10
No. of the volumes/prices of red. scenarios of aggregators	10
No. of the volumes/prices of red. scenarios of ADSO	10
No. of red. scenarios of demand response	10
No. of red. scenarios of day-ahead demands	15
No. of red. scenarios of day-ahead intermittent generation	10
No. of red, scenarios of ADSO external shocks	10

$$SOC_{\max}^{cPHEV} \leqslant SOC \leqslant SOC_{\min}^{cPHEV} \tag{2}$$

$$-P_{max}^{cPHEV}\cdot\gamma^{ch} \leqslant P^{cPHEV} \leqslant P_{max}^{cPHEV}\cdot\gamma_{i,t}^{dch} \tag{3}$$

$$-P_{max}^{cPHEV}\cdot\gamma^{ch} \leqslant P^{cPHEV} \leqslant P_{max}^{cPHEV}\cdot\gamma_{i,t}^{dch} \tag{4}$$

$$E_t^{cPHEV} = E_{t-1}^{cPHEV} - T_p\cdot P_t^{cPHEV}\cdot\left(\gamma_t^{dch}/\pi_{dch}^{cPHEV} + \gamma_t^{ch}\cdot\pi_{ch}^{cPHEV}\right) \tag{5}$$

$$E_{min}^{cPHEV} \leqslant E^{cPHEV} \leqslant E_{max}^{cPHEV} \tag{6}$$

$$E_t^{PHEV} = E_{desire}^{PHEV} \qquad \forall t = t_{departure} \tag{7}$$

2.1.2. The SDERs and parking lots Day-Ahead optimization objective functions

The objective function regarding the optimization of SDERs and parking lots is given as (8):

$$Max\ \mathbb{F}_{\Omega}^{DA} = \sum_{SDEROS} prob\cdot\left(\alpha_{\Omega}^{SR\_DA}\cdot SR_{\Omega}^{DA} + \alpha_{\Omega}^{AP\_DA}\cdot P_{\Omega}^{DA} + \alpha_{\Omega}^{RP\_DA}\cdot Q_{\Omega}^{DA} + \alpha_{\Omega}^{RR\_DA}\cdot RR_{\Omega}^{DA} - C_{\Omega}^{DA}\right)\ \forall\Omega \in SDERs \cap PLs \tag{8}$$

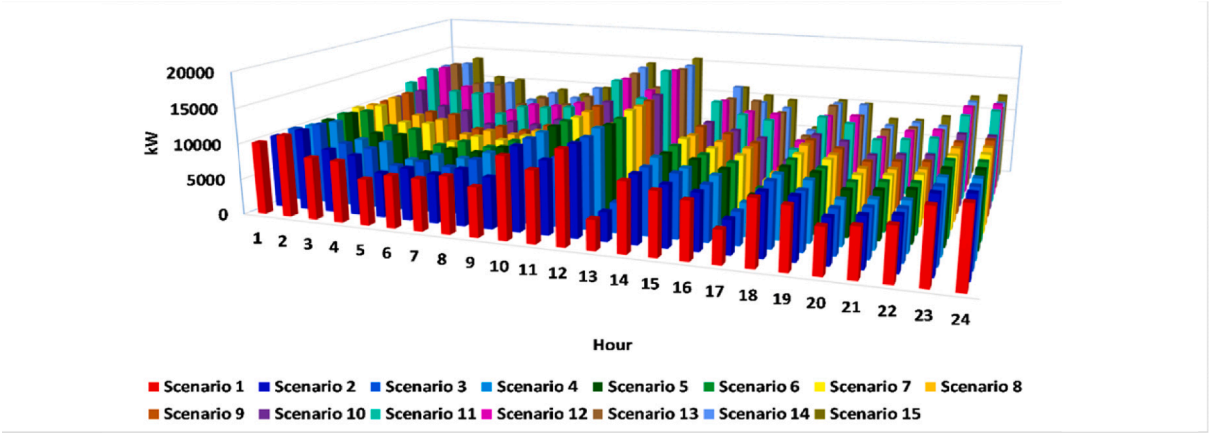

Fig. 5. The day-ahead forecasted electrical load for different scenarios.

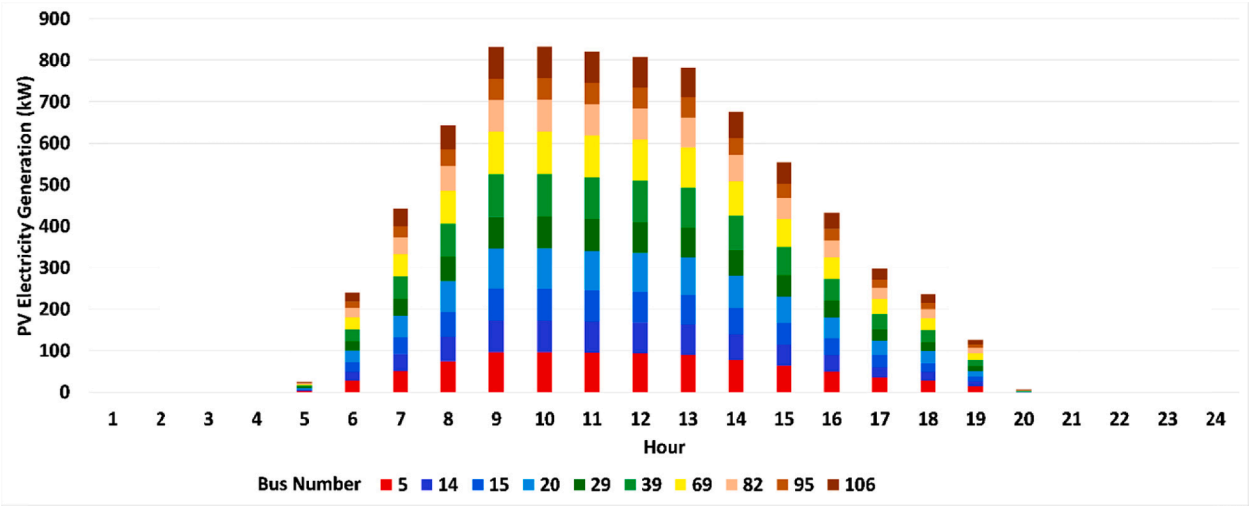

Fig. 6. The forecasted photovoltaic systems electricity generation.

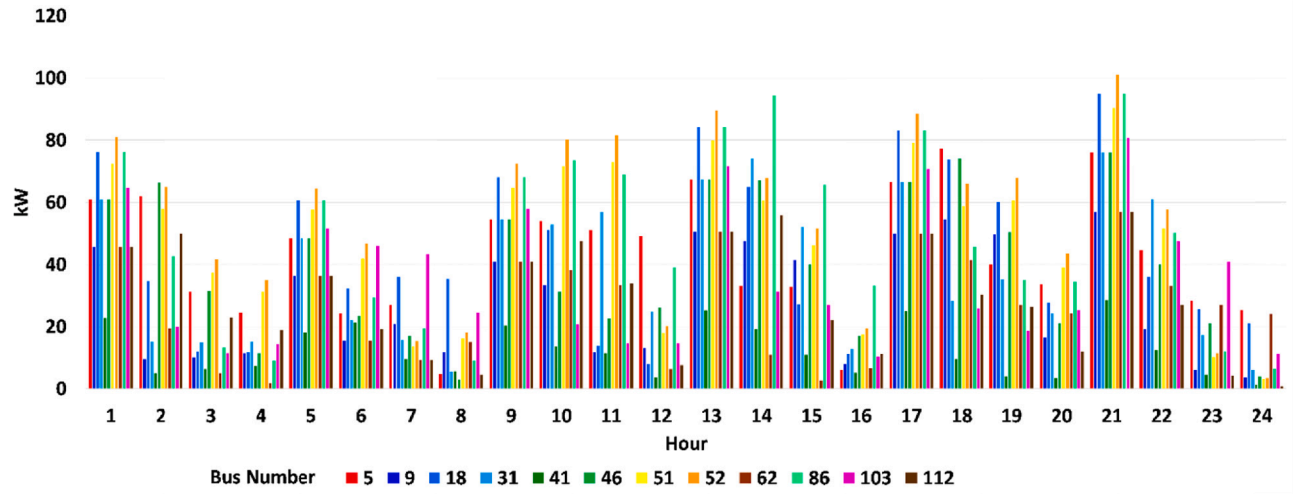

Fig. 7. The forecasted wind turbines' electricity generation.

The C_{Ω}^{DA} is the day-ahead operating cost of the Ω that is categorized into the CHPs, SHs, WTs, PVs, PLs, DGs, and ESSs operating costs, and their detailed formulations are available in [36]. The SDERs and PLs determine the values of $\alpha_{\Omega}^{SR\_DA}, \alpha_{\Omega}^{AP\_DA}, \alpha_{\Omega}^{RP\_DA}, \alpha_{\Omega}^{RR\_DA}$, based on historical data. Eq. (8) can be approximately maximized by the SDERs and PLs. The aggregators determine the values of $SR_{\Omega}^{DA}, P_{\Omega}^{DA}, Q_{\Omega}^{DA}, RR_{\Omega}^{DA}$. Then, the accepted values of $SR_{\Omega}^{DA}, P_{\Omega}^{DA}, Q_{\Omega}^{DA}, RR_{\Omega}^{DA}$ are sent to SDERs and PLs by the corresponding aggregators. Finally, Eq. (8) can be accurately maximized

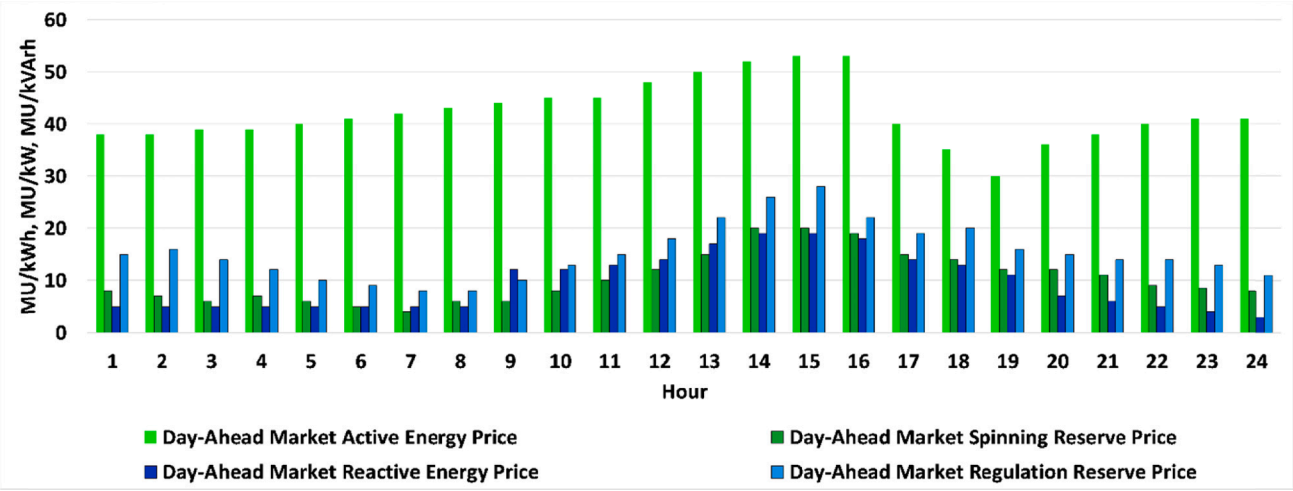

Fig. 8. The day-ahead forecasted price for active power and ancillary services.

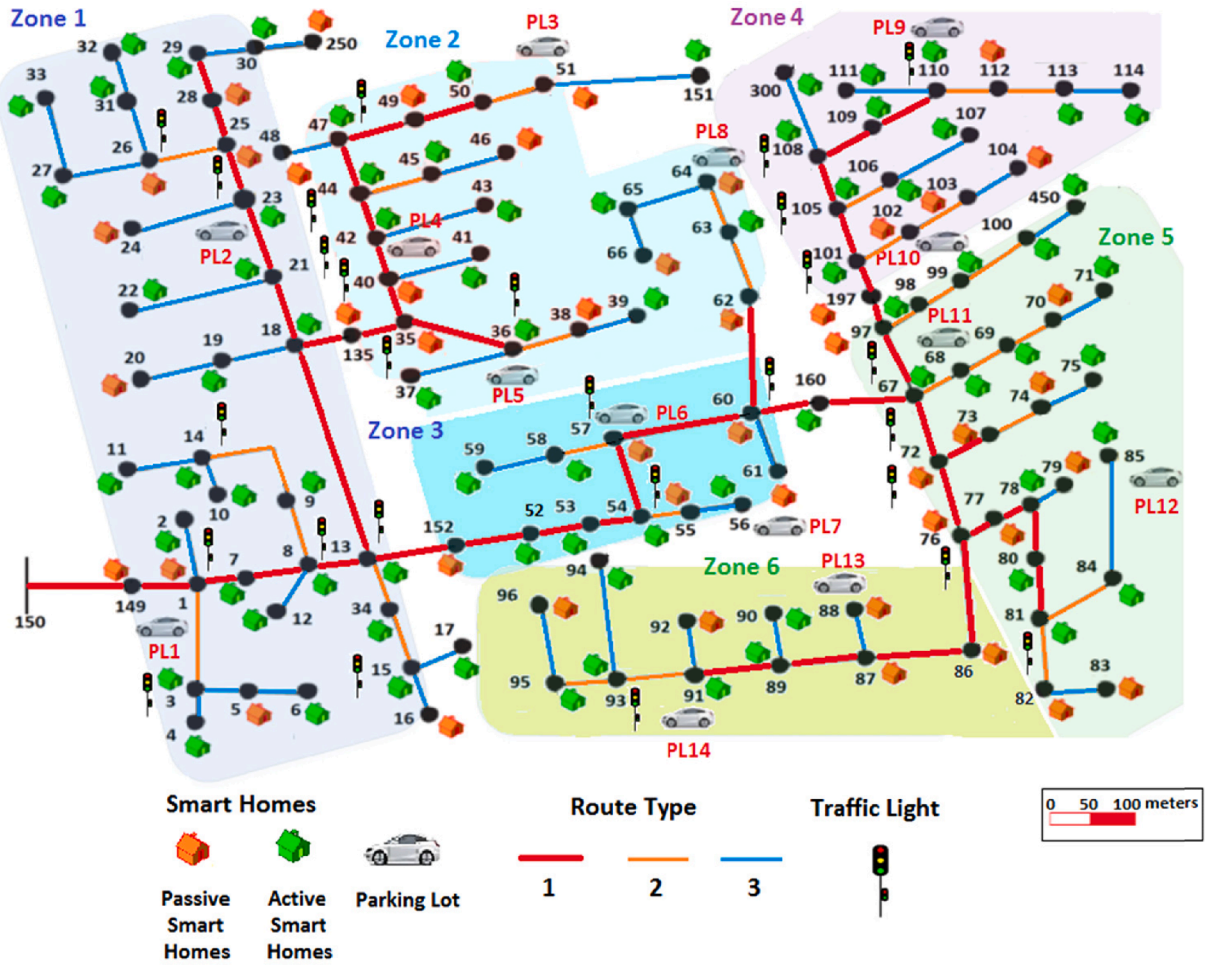

Fig. 9. The topology of the transportation system and the location of traffic lights.

Table 3
The speed limit and traffic light duration of routes.

Route type	1	2	3
Maximum speed limit (m/s)	18	13	11
Traffic light duration (min)	3	2	1

Table 4
The output data for one of the reduced scenarios of PHEV arrival and departures.

Route type	1	2	3
Average speed (m/s) on the routes	8.56	7.79	7.11
Congested routes' traffic duration for 24 h simulation (min)	632	391	377

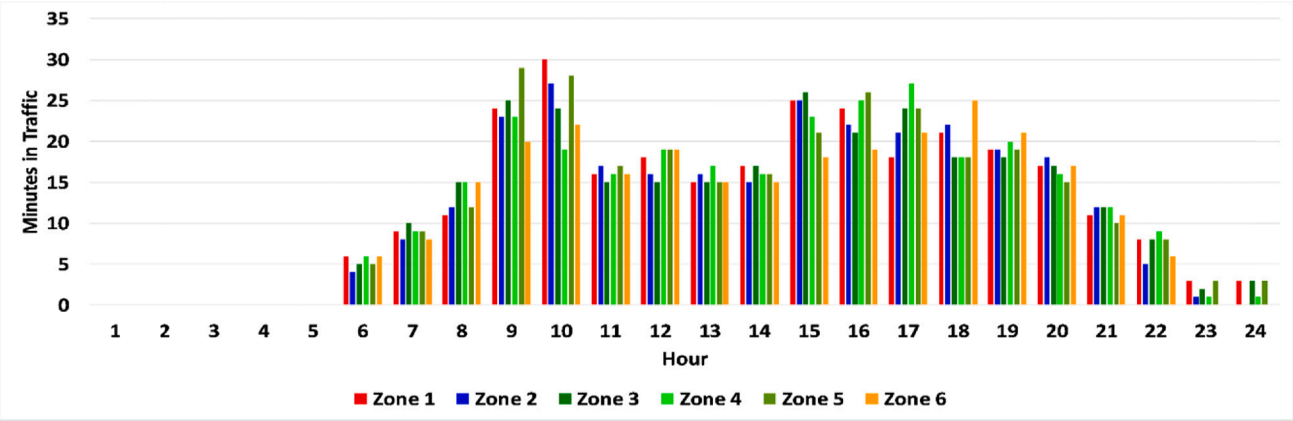

Fig. 10. The estimated average values of durations that vehicles may stay in traffic for different zones of the system.

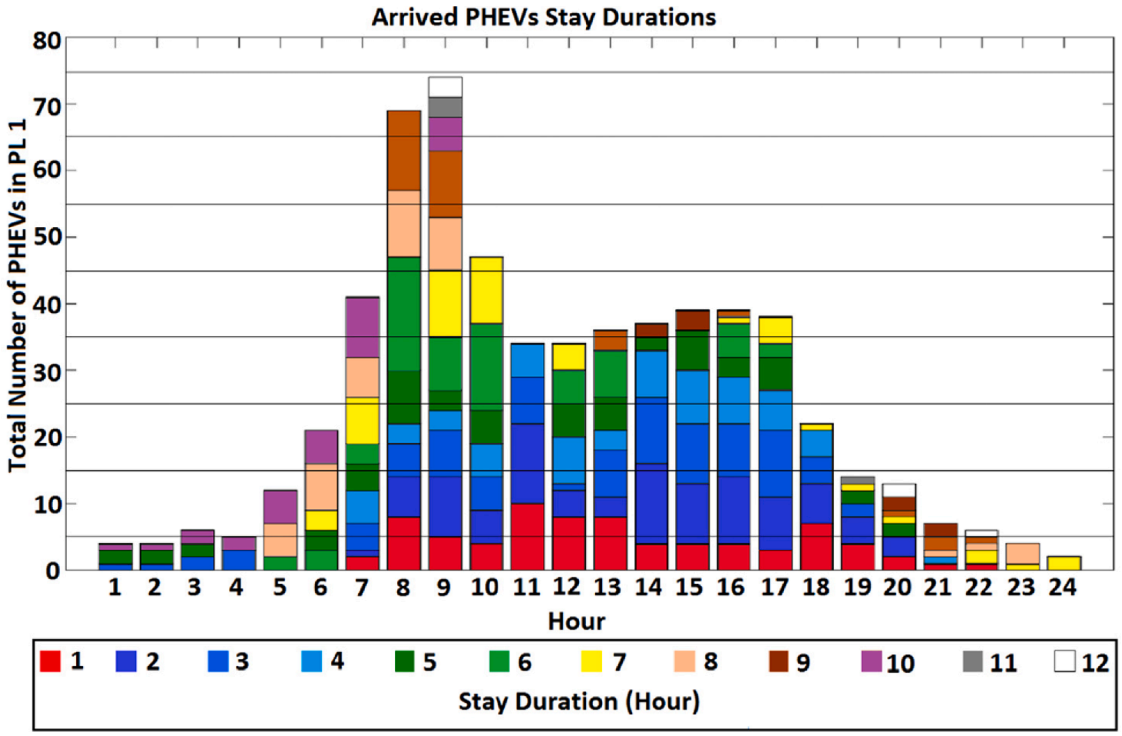

Fig. 11. Stay duration of PHEVs in parking lot 1.

by the PLs and SDERs.

The SDERs and parking lots' day-ahead optimization objective function objective consists of: 1) revenue of spinning reserve offered to the aggregator ($\alpha_{\Omega}^{SR\_DA} \cdot SR_{\Omega}^{DA}$); 2) the revenue of active power sold to the aggregator ($\alpha_{\Omega}^{AP\_DA} \cdot P_{\Omega}^{DA}$); 3) the revenue of reactive power sold to the aggregator ($\alpha_{\Omega}^{RP\_DA} \cdot Q_{\Omega}^{DA}$); 4) the revenue of regulating reserve sold to the aggregator ($\alpha_{\Omega}^{RR\_DA} \cdot RR_{\Omega}^{DA}$); 5) and the operating costs of Ω (C_{Ω}^{DA}).

The day-ahead operating costs of parking lots are compromised by the following terms: 1) cost of spinning reserve purchased from the cPHEVs ($\alpha_{cPHEV}^{SR\_DA} \cdot SR_{cPHEV}^{DA}$); 2) cost of active power purchased from the cPHEVs ($\alpha_{cPHEV}^{AP\_DA} \cdot P_{cPHEV}^{DA}$); 3) and cost of regulating reserve purchased from the cPHEVs ($\alpha_{cPHEV}^{RR\_DA} \cdot RR_{cPHEV}^{DA}$). The penalties of mismatches of cPHEV day-ahead and real-time active power generations ($\sum Penalty_{cPHEV}$) are considered as the benefit of parking lots.

Eq. (8) is subject to the following constraints:

$$P_{min}^{DG} \cdot I \leqslant P^{DG} \leqslant P_{max}^{DG} \cdot I \tag{9}$$

$$\left|\left(P_t^{DG} - P_{t-1}^{DG}\right)\right| \leqslant \Delta U^{DG} \tag{10}$$

$$SOC_{\min} \leqslant SOC \leqslant SOC_{\max} \tag{11}$$

Where, SOC is the state of the charge of the ESS. The state of charge of energy storage in the t^{th} simulation step can be written as (12):

$$SOC_t = SOC_{t-1} - \frac{T_p \cdot P_t^{ESS}}{cap^{ESS}} \cdot \left(\lambda_t^{ch} \cdot \eta_{ch} + \lambda_t^{dch} \cdot \eta_{dch}^{-1}\right) \tag{12}$$

ESS constraints are given as (13):

$$-P_{max}^{ESS,ch} \cdot \lambda^{ch} \leqslant P^{ESS} \leqslant P_{max}^{ESS,dch} \cdot \lambda^{dch} \tag{13}$$

The constraints of smart home demand response programs are presented as (14):

$$\Delta P_{\min}^{DRP} \leqslant \Delta P_{SH}^{DRP} \leqslant \Delta P_{\max}^{DRP} \tag{14}$$

Where, $\Delta P_{\min}^{DRP}$ and $\Delta P_{\max}^{DRP}$ are the minimum/maximum load changes in the demand response process of the smart home, respectively. The

detailed formulation of WT, CHP, and PV constraints is available in [36]. The parking lot objective function is constrained by the following equation:

$$P^{PL} = (-\sum P^{cPHEV} - P^{PL\ Loss} + P^{PL\ IMPORT}) \quad (15)$$

Where, $P^{PL\ Loss}$ and $P^{PL\ IMPORT}$ are the parking lot electrical loss and the imported active power, respectively.

2.1.3. The aggregator Day-Ahead optimization objective function

The objective function of the aggregators is given as (16):

$$Max\ \mathbb{F}^{\mathrm{DA}}_{\mathrm{AGG}} = \sum_{\mathrm{AGGS}} \mathrm{prob}\cdot(\alpha^{\mathrm{SR\_DA}}_{\mathrm{AGG}}\cdot \mathrm{SR}^{\mathrm{SR\_DA}}_{\mathrm{AGG}} + \alpha^{\mathrm{AP\_DA}}_{\mathrm{AGG}}\cdot \mathrm{P}^{\mathrm{DA}}_{\mathrm{AGG}} + \alpha^{\mathrm{RP\_DA}}_{\mathrm{AGG}}\cdot \mathrm{Q}^{\mathrm{DA}}_{\mathrm{AGG}} + \alpha^{RR\_DA}_{AGG}\cdot RR^{DA}_{AGG} - C^{DA}_{AGG}) \quad (16)$$

The day-ahead operating cost of aggregator (C^{DA}_{AGG}) is compromised by the subsequent terms: 1) costs of spinning reserve purchased from SDERs and PLs ($\alpha^{SR\_DA}_{\Omega}\cdot SR^{DA}_{\Omega}$); 2) costs of active power purchased from SDERs and PLs ($\alpha^{AP\_DA}_{\Omega}\cdot P^{DA}_{\Omega}$); 3) costs of reactive power purchased from SDERs and PLs ($\alpha^{RP\_DA}_{\Omega}\cdot Q^{DA}_{\Omega}$); 4) and costs of regulating reserve purchased from SDERs and PLs ($\alpha^{RR\_DA}_{\Omega}\cdot RR^{DA}_{\Omega}$).

Eq. (16) is subjected to the electric power balance constraint that is given by (17):

$$P^{AGG} = (-\sum P^{Load} + \sum P^{PV} + \sum P^{ESS} + \sum P^{CHP} + \sum P^{WT} \pm \sum P^{DRP} \pm \sum P^{PL}) \quad (17)$$

Where, P^{AGG},P^{Load},P^{PV}, P^{ESS},P^{CHP},P^{WT},P^{DRP} , and P^{PL} are the active power of the aggregator, the active power of load, the active power of photovoltaic arrays, the active power of ESS, the active power of CHP, the active power of wind turbine, the active power of demand response process, and the active power of parking lot, respectively. The aggregator can contract with the smart homes to perform Direct Load Control (DLC). The demand response process constraints are [36]:

$$P^{DRP} = \Delta P^{DLC} = P^{Load}_{Controllable} \quad (18)$$

$$\Delta P^{DLC}_{Min} \leqslant \Delta P^{DLC} \leqslant \Delta P^{DLC}_{Max} \quad (19)$$

Eq. (18) presents that the demand response process is carried out for controllable loads of smart homes. Eq. (19) denotes the max/min restrictions of direct load control variables.

2.1.4. The ADSO Day-Ahead optimization objective function

The objective function regarding the ADSO is given as (20):

$$Max\ \mathbb{F}^{\mathrm{Normal\_DA}}_{\mathrm{ADSO}} = \sum_{\mathrm{ADSOS}} \mathrm{prob}\cdot(\alpha^{\mathrm{SR\_DA}}_{\mathrm{ADSO}}\cdot \mathrm{SR}^{\mathrm{SR\_DA}}_{\mathrm{ADSO}} + \alpha^{\mathrm{AP\_DA}}_{\mathrm{ADSO}}\cdot \mathrm{P}^{\mathrm{DA}}_{\mathrm{ADSO}} + \alpha^{\mathrm{RP\_DA}}_{\mathrm{ADSO}}\cdot \mathrm{Q}^{\mathrm{DA}}_{\mathrm{ADSO}} + \alpha^{RR\_DA}_{ADSO}\cdot RR^{DA}_{ADSO} - C^{DA}_{ADSO}) + [(\gamma^{-R}\cdot P^{RT}_{ADSO} + u') + \Theta\Gamma] \quad (20)$$

The ADSO day-ahead optimization objective function objective consists of the following terms: 1) revenue of spinning reserve sold to the upward electricity market ($\alpha^{SR\_DA}_{ADSO}\cdot SR^{DA}_{ADSO}$); 2) revenue of active power sold to the upward electricity market ($\alpha^{AP\_DA}_{ADSO}\cdot P^{DA}_{ADSO}$); 3) revenue of reactive power sold to the upward electricity market ($\alpha^{RP\_DA}_{ADSO}\cdot Q^{DA}_{ADSO}$); 4) revenue of regulating reserve sold to the upward electricity market ($\alpha^{RR\_DA}_{ADSO}\cdot RR^{DA}_{ADSO}$); 5) operating costs of aggregator (C^{DA}_{ADSO}); 6) and expected value of revenue in the real-time market and the robustness parameter $[(\gamma^{-R}\cdot P^{RT}_{ADSO} + u') + \Theta\Gamma]$.

The day-ahead operating cost of ADSO (C^{DA}_{ADSO}) is compromised by the following terms: 1) cost of spinning reserve purchased from aggregators ($\alpha^{SR\_DA}_{AGG}\cdot SR^{DA}_{AGG}$); 2) cost of active power purchased from aggregators ($\alpha^{AP\_DA}_{AGG}\cdot P^{DA}_{AGG}$); 3) cost of reactive power purchased from aggregators ($\alpha^{RP\_DA}_{AGG}\cdot Q^{DA}_{AGG}$); 4) and cost of regulating reserve purchased from aggregators ($\alpha^{RR\_DA}_{AGG}\cdot RR^{DA}_{AGG}$). Eq. (20) is subjected to the following constraints:

2.2. Electric power balance constraint

The electric power balance constraint is given by (21):

$$P^{ADSO} = (\sum P^{AGG} \mp \sum P^{MTRAN} - P^{Loss}) \quad (21)$$

Where, P^{AGG}, P^{MTRANS}, and P^{Loss} are active power of the aggregator, active power transaction with the upward market, and active power loss in the electrical system of ADSO, respectively.

2.3. Security Constraints:

$$\sqrt{P^2_{ADSO\_LINE} + Q^2_{ADSO\_LINE}} \leqslant F^{\mathrm{Max}}_{ADSO\_LINE} \quad (22)$$

$$V^{\min} \leqslant |V| \leqslant V^{\max} \quad (23)$$

Eq. (22) terms are the active (P_{ADSO_LINE}) and reactive power (Q_{ADSO_LINE}) of the ADSO feeders. At the day-ahead optimization problem, the ADSO simulates the sectionalizing process of the distribution system into multi-microgrids to mitigate the impact of external shock. Thus, the objective function of the day-ahead optimization process of ADSO in the simulation process of external shock conditions can be written as (24):

$$Min\ \mathbb{F}^{\mathrm{Ext\_Shock\_DA}}_{\mathrm{ADSO}} = \sum_{\mathrm{ADSOEXS}} \mathrm{prob}\cdot(\mathrm{W}_1\cdot \mathrm{C}^{\mathrm{Ext\_Shock\_DA}}_{\mathrm{ADSO}} + \mathrm{W}_2\cdot \mathrm{RI} + \mathrm{W}_3\cdot \sum_{\mathrm{NBL}} \mathrm{X}) \quad (24)$$

Where, *ADSOEXS* is the set of the operating scenario of the ADSO in external shock conditions. In (24), the $C^{Ext\_Shock\_DA}_{ADSO}$ is the operating cost of the ADSO in external shock conditions. *NBL* is the set of boundary lines [1].

The ADSO utilizes a Resiliency Index (RI) to assess the level of resiliency of the system in the worst-case conditions. The RI is defined as (25):

Table 5
The estimated values of the number of arrived PHEVs, the number of departed PHEVs, the capacity of departed PHEVs, and the available capacity of PHEVs in parking lot 1 for one of the reduced scenarios.

Time	Number of Arrived PHEVs	Number of Departed PHEVs	The Capacity of Departed PHEVs (kW)	Number of Available PHEVs in Parking Lot	The Available Capacity of Parking Lot 1 (kW)
1	**4**	**0**	**0**	**4**	**28**
2	**4**	**0**	**0**	**8**	**56**
3	**6**	**0**	**0**	**14**	**98**
4	**5**	**0**	**0**	**19**	**133**
5	**12**	**0**	**0**	**31**	**217**
6	**21**	**1**	**35**	**51**	**357**
7	**41**	**0**	**0**	**92**	**644**
8	**69**	**7**	**245**	**154**	**1078**
9	**74**	**15**	**525**	**213**	**1491**
10	**47**	**17**	**595**	**243**	**1701**
11	**31**	**24**	**840**	**250**	**1750**
12	**29**	**29**	**1015**	**250**	**1750**
13	**32**	**32**	**1120**	**250**	**1750**
14	**37**	**37**	**1295**	**250**	**1750**
15	**39**	**39**	**1365**	**245**	**1715**
16	**39**	**37**	**1295**	**229**	**1603**
17	**38**	**38**	**1330**	**200**	**1400**
18	**22**	**22**	**770**	**165**	**1155**
19	**14**	**14**	**490**	**128**	**896**
20	**13**	**13**	**455**	**93**	**651**
21	**7**	**7**	**245**	**70**	**490**
22	**6**	**6**	**210**	**52**	**364**
23	**4**	**4**	**140**	**39**	**273**
24	**2**	**2**	**70**	**33**	**231**

$$RI = \frac{\sum \textit{Served Electrical Loads in Contingent Conditions}}{\sum \textit{Served Electrical Loads in Normal Conditions} - \sum \textit{Served Electrical Loads in Contingent Conditions}} \tag{25}$$

The RI tends to the infinite when all of the system's loads are supplied in the contingent conditions. The RI is calculated for N-K contingencies that are determined by the ADSO.

Eq. (24) consists of the following terms: 1) the operating cost of the ADSO in external shock conditions ($C_{ADSO}^{Ext\_Shock\_DA}$); 2) the resiliency index (RI); 3) and the boundary lines of multi-microgrids [1]. W is the weighting factor.

2.4. The Real-Time optimization problems

2.4.1. The cPHEV Real-Time optimization objective function

The cPHEV owner maximizes his/her profits in the real-time ramp market. The EVEMS receives real-time traffic signals and determines the estimated values of energy consumption (ς_{Fuel}) and change in SOC of cPHEV (ΔSOC) for a probable trip. The objective function of cPHEVs is given as (26):

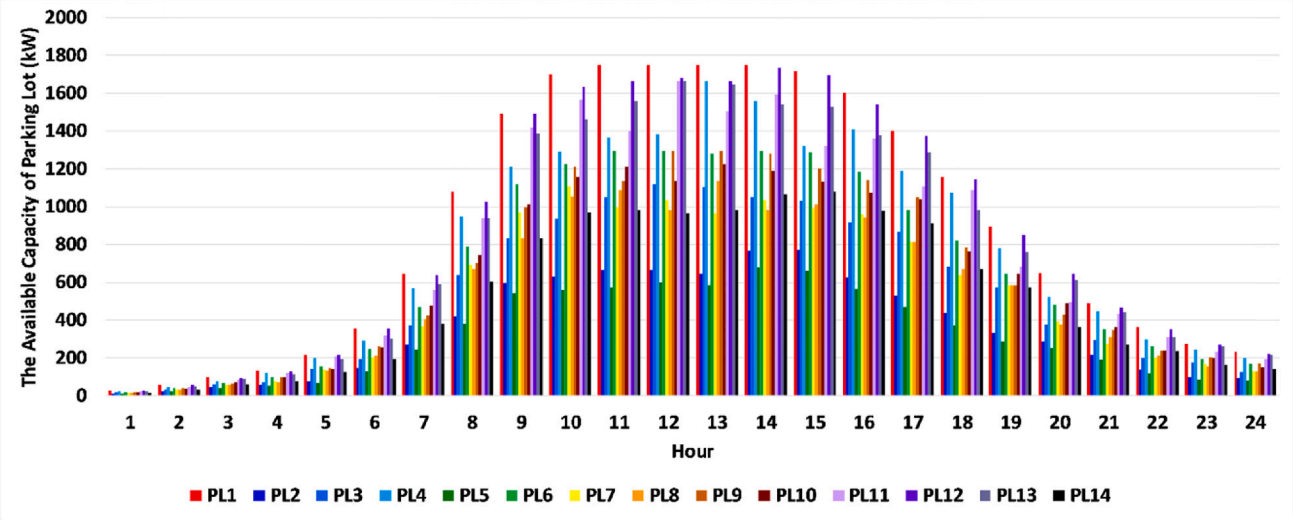

Fig. 12. The estimated values of the available capacity of PHEVs in the parking lots for one of the reduced scenarios.

$$Max\ \mathbb{Z}^{RT}_{cPHEV} = \sum_{t=0}^{T}(\beta^{AP\_RT}_{cPHEV}\cdot P^{RT}_{cPHEV} + \beta^{RAMP^+}_{cPHEV}\cdot P^{RAMP^+}_{cPHEV} + \beta^{RAMP^-}_{cPHEV}\cdot P^{RAMP^-}_{cPHEV} - c^{RT}_{cPHEV}\cdot P^{RT}_{cPHEV} - c^{RAMP^-}_{cPHEV}\cdot P^{RAMP^-}_{cPHEV} - c^{RAMP^+}_{cPHEV}\cdot P^{RAMP^+}_{cPHEV} - \zeta_{Fuel}\cdot\lambda_{Fuel} - \varpi_{cPHEV}\cdot\Delta SOC\cdot\beta^{AP\_RT}_{Agg}) \quad (26)$$

The EVEMS determines the values of $\beta^{AP\_RT}_{cPHEV}, \beta^{RAMP^+}_{cPHEV}, \beta^{RAMP^-}_{cPHEV}$ based on historical data [13,14]. Eq. (26) can be approximately maximized by the EVEMS considering the estimated values of P^{RT}_{cPHEV}, $P^{RAMP^+}_{cPHEV}, P^{RAMP^-}_{cPHEV}$. Then, the parking lot optimization process should determine the values of P^{RT}_{cPHEV}, $P^{RAMP^+}_{cPHEV}, P^{RAMP^-}_{cPHEV}$ variables. Finally, the accepted values of P^{RT}_{cPHEV}, $P^{RAMP^+}_{cPHEV}, P^{RAMP^-}_{cPHEV}$ variables are sent to PHEVs by the corresponding PLs and the value of Eq. (26) can be accurately maximized by the EVEMSs. Eq. (26) is subjected to (2) - (7) constraints.

2.4.2. The SDERs and parking lots Real-Time optimization objective function

The general form of objective functions of the SDERs and parking lots

$$Max\ \mathbb{Z}^{RT}_{ADSO} = \sum_{t=0}^{T}(\beta^{AP\_RT}_{ADSO}\cdot P^{RT}_{ADSO} + \beta^{RP\_RT}_{ADSO}\cdot Q^{RT}_{ADSO} + \beta^{RAMP^+}_{ADSO}\cdot P^{RAMP^+}_{ADSO} + \beta^{RAMP^-}_{ADSO}\cdot P^{RAMP^-}_{ADSO} - c^{RT}_{ADSO} - c^{RAMP^-}_{ADSO} - c^{RAMP^+}_{ADSO}) \quad (29)$$

can be written as (27):

$$Max\ \mathbb{Z}^{RT}_{\Omega} = \sum_{t=0}^{T}(\beta^{AP\_RT}_{\Omega}\cdot P^{RT}_{\Omega} + \beta^{RP\_RT}_{\Omega}\cdot Q^{RT}_{\Omega} + \beta^{RAMP^+}_{\Omega}\cdot P^{RAMP^+}_{\Omega} + \beta^{RAMP^-}_{\Omega}\cdot P^{RAMP^-}_{\Omega} - c^{RT}_{\Omega} - c^{RAMP^-}_{\Omega} - c^{RAMP^+}_{\Omega})\ \forall\Omega\in SDER\cap PL \quad (27)$$

The real-time operating costs of parking lots are compromised by the following terms: 1) the cost of active power purchased from cPHEVs ($\beta^{RT}_{cPHEV}\cdot P^{RT}_{cPHEV}$); 2) the cost of ramp-up ancillary service purchased from cPHEVs ($\beta^{RAMP^+}_{cPHEV}\cdot P^{RAMP^+}_{cPHEV}$); 3) and the cost of ramp-down ancillary service purchased from cPHEVs ($\beta^{RAMP^-}_{cPHEV}\cdot P^{RAMP^-}_{cPHEV}$). The SDERs and PLs optimization processes determine the values of $\beta^{AP\_RT}_{\Omega}, \beta^{RP\_RT}_{\Omega}, \beta^{RAMP^+}_{\Omega}, \beta^{RAMP^-}_{\Omega}$ based on historical data. Eq. (27) can be approximately maximized by the SDERs and PLs. The aggregators should determine the values of $P^{RT}_{\Omega}, Q^{RT}_{\Omega}$, $P^{RAMP^+}_{\Omega}, P^{RAMP^-}_{\Omega}$. Then, the accepted values of $P^{RT}_{\Omega}, Q^{RT}_{\Omega}$, $P^{RAMP^+}_{\Omega}, P^{RAMP^-}_{\Omega}$ are sent to SDERs and PLs by the corresponding aggregators. Finally, Eq. (27) can be accurately maximized by the PLs and SDERs. Eq. (27) is subjected to (9) - (15).

2.4.3. The aggregator Real-Time optimization objective function

The objective function of the aggregator is given as (28):

$$Max\ \mathbb{Z}^{RT}_{AGG} = \sum_{t=0}^{T}(\beta^{AP\_RT}_{AGG}\cdot P^{RT}_{AGG} + \beta^{RP\_RT}_{AGG}\cdot Q^{RT}_{AGG} + \beta^{RAMP^+}_{AGG}\cdot P^{RAMP^+}_{AGG} + \beta^{RAMP^-}_{AGG}\cdot P^{RAMP^-}_{AGG} - c^{RT}_{AGG} - c^{RAMP^-}_{AGG} - c^{RAMP^+}_{AGG}) \quad (28)$$

The aggregators determine the values of $\beta^{AP\_RT}_{AGG}, \beta^{RP\_RT}_{AGG}, \beta^{RAMP^+}_{AGG}, \beta^{RAMP^-}_{AGG}$ based on historical data. Eq. (28) can be approximately maximized by the aggregator considering the estimated values of $P^{RAMP^+}_{AGG}, P^{RAMP^-}_{AGG}, P^{RT}_{AGG}$, Q^{RT}_{AGG}. Then, the ADSO determines the values of $P^{RAMP^+}_{AGG}, P^{RAMP^-}_{AGG}, P^{RT}_{AGG}, Q^{RT}_{AGG}$ variables. Finally, the accepted values of $P^{RAMP^+}_{AGG}, P^{RAMP^-}_{AGG}, P^{RT}_{AGG}, Q^{RT}_{AGG}$ variables are sent to the aggregator by the ADSO and the value of Eq. (28) can be accurately maximized by the aggregators.

The real-time operating cost of aggregator (c^{RT}_{AGG}) consists of the subsequent terms: 1) the cost of active power purchased from SDERs and PLs ($\beta^{AP\_RT}_{\Omega}\cdot P^{RT}_{\Omega}$); 2) the cost of reactive power purchased from SDERs and PLs ($\beta^{RP\_RT}_{\Omega}\cdot Q^{RT}_{\Omega}$); 3) the cost of ramp-up ancillary service purchased from SDERs and PLs ($\beta^{RAMP^+}_{\Omega}\cdot P^{RAMP^+}_{\Omega}$); 4) and the cost of ramp-down ancillary service purchased from SDERs and PLs ($\beta^{RAMP^-}_{\Omega}\cdot P^{RAMP^-}_{\Omega}$). Eq. (28) is subjected to (17) - (19) constraints.

2.4.4. ADSO Real-Time optimization objective function

The objective function regarding the ADSO is given as (29):

The ADSO optimization process determines the values of $\beta^{AP\_RT}_{ADSO}$, $\beta^{RP\_RT}_{ADSO}, \beta^{RAMP^+}_{ADSO}, \beta^{RAMP^-}_{ADSO}$ and Eq. (29) can be approximately maximized by the ADSO. The wholesale market operator should determine the values of $P^{RT}_{ADSO}, Q^{RT}_{ADSO}$, $P^{RAMP^+}_{ADSO}, P^{RAMP^-}_{ADSO}$. Finally, Eq. (29) can be accurately maximized by the ADSO. Eq. (29) optimization objective function objective consists of the following terms: 1) revenue of active power sold to the upward market ($\beta^{AP\_RT}_{ADSO}\cdot P^{RT}_{ADSO}$); 2) revenue of reactive power sold to the upward market ($\beta^{RP\_RT}_{ADSO}\cdot Q^{RT}_{ADSO}$); 3) revenue of ramp-up ancillary service sold to the upward market ($\beta^{RAMP^+}_{ADSO}\cdot P^{RAMP^+}_{ADSO}$); 4) revenue of ramp-down ancillary service offered to upward market ($\beta^{RAMP^-}_{ADSO}\cdot P^{RAMP^-}_{ADSO}$); 5) real-time operating cost of ADSO (c^{RT}_{ADSO}); 6) cost of ramp-down ancillary service ($c^{RAMP^-}_{ADSO}$) ; 7) and cost of ramp-up ancillary service ($c^{RAMP^+}_{ADSO}$).

The real-time operating cost of ADSO (c^{RT}_{ADSO}) is compromised by the following terms: 1) the cost of active power purchased from aggregators ($\beta^{AP\_RT}_{AGG}\cdot P^{RT}_{AGG}$); 2) the cost of reactive power purchased from aggregators ($\beta^{RP\_RT}_{AGG}\cdot Q^{RT}_{AGG}$); 3) the ramp-up ancillary service cost purchased from aggregators ($\beta^{RAMP^+}_{AGG}\cdot P^{RAMP^+}_{AGG}$); 4) ramp-down ancillary service cost purchased from aggregators ($\beta^{RAMP^-}_{AGG}\cdot P^{RAMP^-}_{AGG}$).

Eq. (29) is subjected to (21) - (23) constraints.

The objective function in the external shock conditions is given as (30):

$$Min\ \mathbb{F}^{\text{Ext\_Shock\_RT}}_{\text{ADSO}} = \mathrm{W}'_1\cdot\mathrm{C}^{\text{Ext\_Shock\_RT}}_{\text{ADSO}} + \mathrm{W}'_2\cdot\sum_{\text{NBL}}\mathrm{X} + \mathrm{W}'_3\cdot\sum_{\text{NCU}}\mathrm{CIC} \quad (30)$$

In (30), $C^{Ext\_Shock\_RT}_{ADSO}$ is the operating cost of the ADSO in external shock conditions. The process endeavors to minimize the power that flows through boundary lines. It is assumed that each boundary line is equipped with normally closed sectionalizer switches.

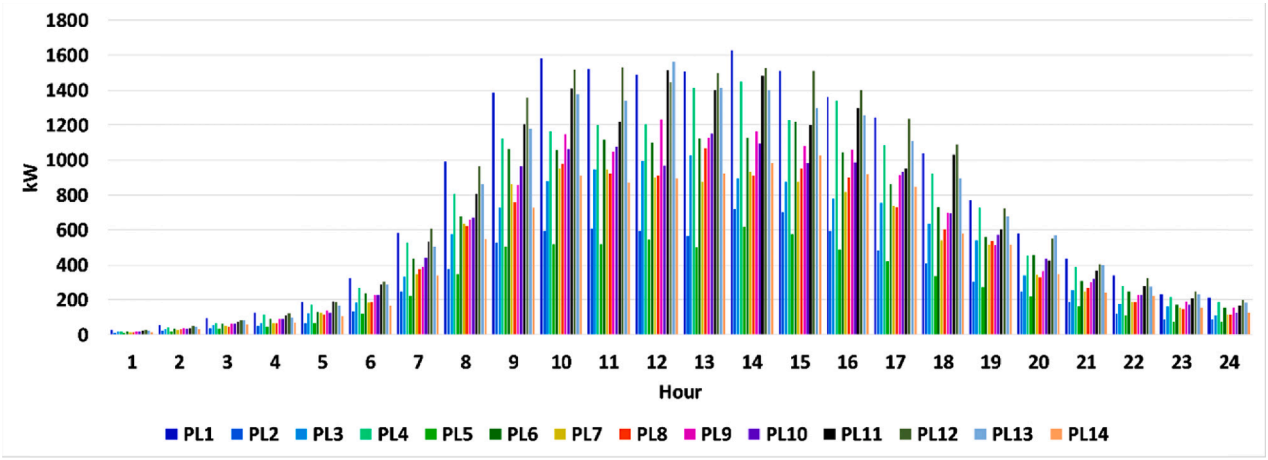

(a)

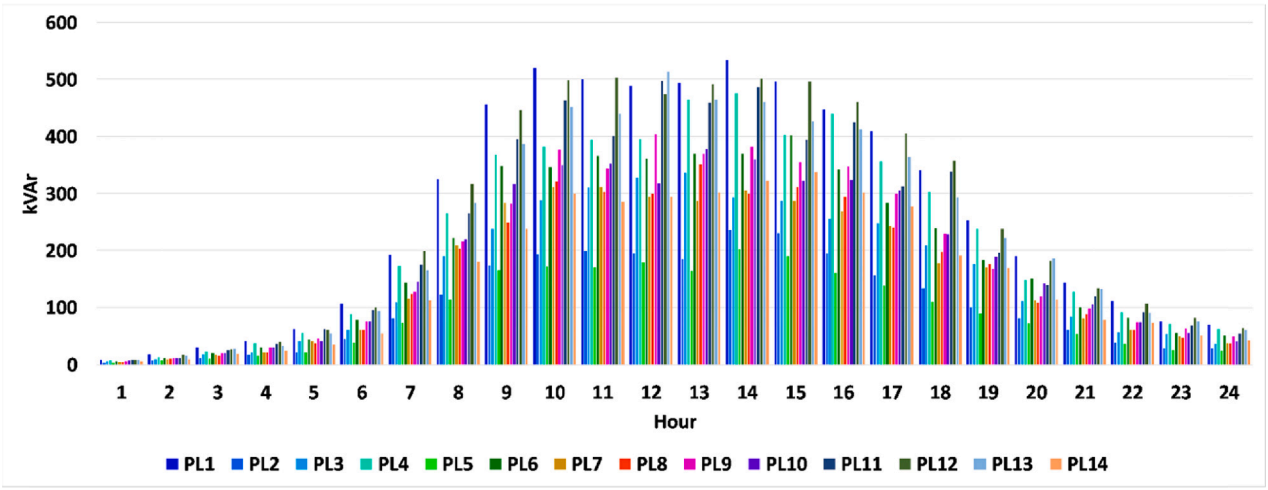

(b)

Fig. 13. (a) The accepted values of active power, (b) reactive power, (c) spinning reserve, (d) regulating reserve of parking lots.

3. Solution methodology

The proposed approach is an iterative one with two stages and four levels. Fig. 3 (a) introduces the day-ahead optimization process of the problem. Fig. 3 (b) depicts the real-time optimization procedure. The uncertainty is modeled using ARIMA model [39–41]. The proposed model compromises continuous, discrete, and non-linear variables. Different MINLP solution methods and GAMS solvers were utilized to solve the proposed model. The optimization codes were developed in GAMS. The traffic simulation process was coded in MATLAB.

4. Simulation results

The 123-bus test system is studied to evaluate the model [36], Fig. 4. The active smart homes are shown in green color and transacting active power with their corresponding aggregator. The scenarios are given in Table 2. Figs. 5, 6, and 7 depict the day-ahead forecasted load, electricity generation of photovoltaic arrays and wind turbines. Fig. 8 presents the prices.

It was assumed that the topology of routes was the same as the 123-bus system topology. Fig. 9 depicts the topology of the transportation system, the location of traffic lights, and the type of routes. Total travel distance was assumed 39531 m based on the scaled map, as shown in Fig. 9. The model of the traffic simulation of Ref. [13] was utilized to generate driving scenarios. Numerous scenarios were generated for the PHEV arrival and departure for the day-ahead optimization process. It was assumed that the PHEVs traveled from smart homes/parking lots to/from parking lots/smart homes for each scenario. Thus, the PHEVs' velocity, departure time, and arrival time were considered as input parameters for each scenario. Then, based on the PHEV arrival and departure scenarios, as shown in Table 2, the scenarios of day-ahead cPHEVs energy consumption and change in SOC based on the forecasted traffic patterns on routes were generated. The mean values for the input parameters of scenarios were the same as the values of Ref. [14]. The simulation snapshot was considered 5 min for the day-ahead problem. It was assumed that when the number of PHEVs was greater than two PHEVs, the corresponding route was recognized as a congested route. Table 3 presents the speed limit and traffic light duration of route data.

Table 4 illustrates the simulation results for one of the reduced

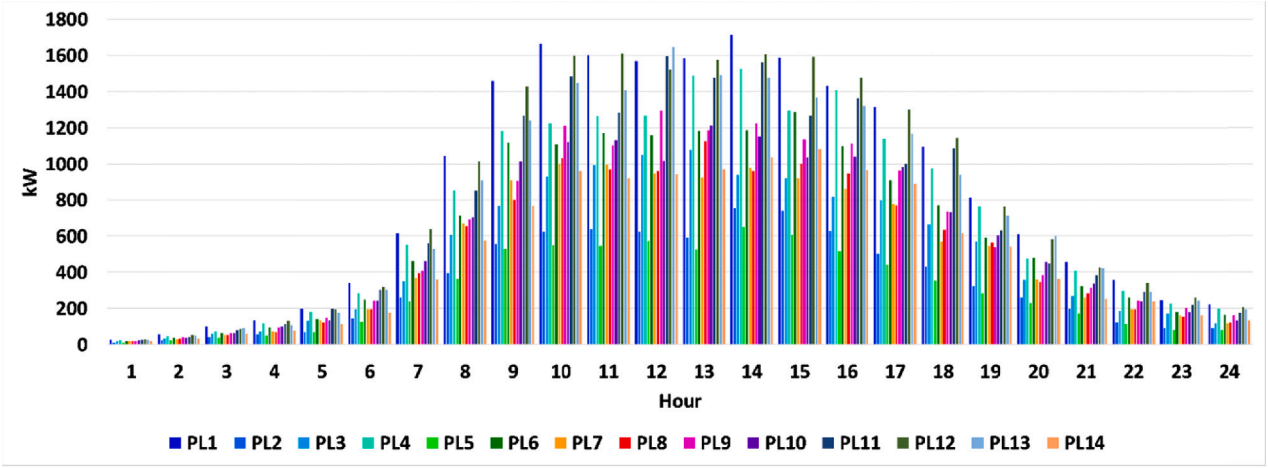

(c)

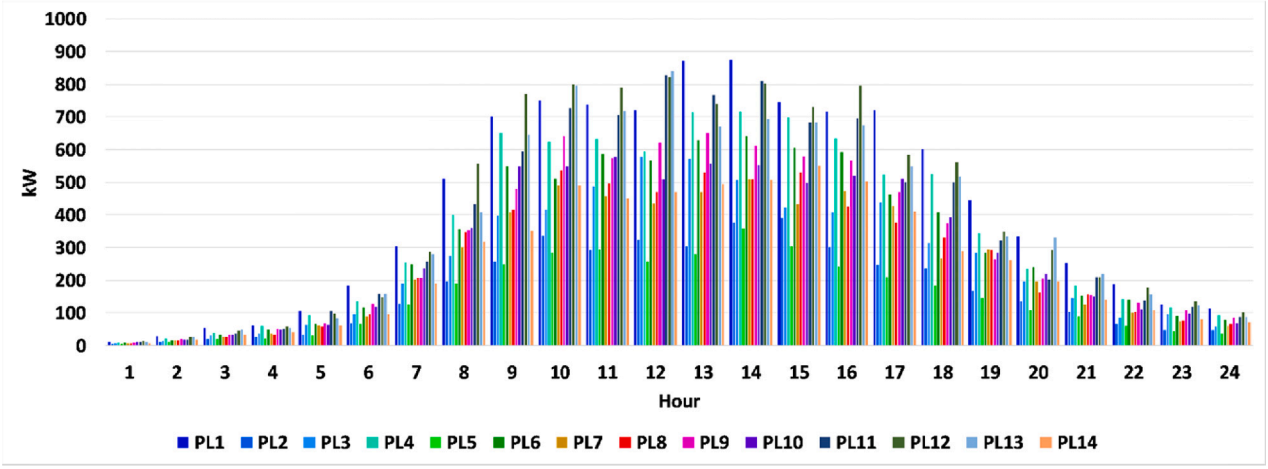

(d)

Fig. 13. (*continued*).

scenarios of PHEV arrival and departures. As shown in Table 4, the average speed of the PHEVs were 8.56 (m/s), 7.79 (m/s), and 7.11 (m/s) for the first, second, and third types of routes, respectively. Further, the congested routes' traffic durations were about 45.14%, 27.92%, and 26.94% for the first, second, and third types of routes, respectively.

Other details of the traffic model are presented in Ref. [13] and are not presented for the sake of space.

Fig. 10 shows the estimated average values of durations in minutes that vehicles may stay in traffic for different zones of the system.

Fig. 11 depicts the estimated values of stay durations of vehicles that may stay in parking lot 1 for one of the reduced scenarios. The maximum stay duration was assumed 12 h. For example, for hour 5, the following vehicles arrived: a) Two vehicles arrive and will stay six hours, b) Five vehicles arrive and will stay eight hours, c) Five vehicles arrive and will stay eight hours. Table 5 presents the estimated values of the number of arrived PHEVs, number of departed PHEVs, capacity of departed PHEVs, the available capacity of PHEVs in PL1 for one of the reduced scenarios.

Fig. 12 shows the estimated values of the available capacity of PHEVs in the parking lots for one of the reduced scenarios. The average and aggregated available capacity of PHEVs were about 630.60 kWh and 211882.17 kWh, respectively.

Fig. 13 (a), (b), (c), and (d) describe the accepted values of power and reserve of parking lots for the day-ahead market. The aggregated value of accepted active power of parking lots was 190651.15 kWh, which was about 89.97% of the available capacity of parking lots. The average values of active power, reactive power, spinning reserve, and regulating reserve of parking lots were about 567.41 kWh, 186.39 kVArh, 597.24 kW, and 299.5 kW, respectively.

Fig. 14 (a) and Fig. 14 (b) depict the accepted values of the active power of smart homes and the energy transactions of ESSs, respectively. The average and aggregated values of smart homes were about 707.3 kWh and 16975.42 kWh, respectively. The average and aggregated value of ESSs were about 578.93 kWh and 13894.33 kWh, respectively.

Fig. 15 (a), (b), (c), and (d) represent the accepted values of active power, reactive power, spinning reserve, and regulating reserve of distributed generation facilities for the day-ahead market, respectively. The aggregated value of the accepted active power of distributed generations was 33616.1 kWh. The average values were around 107.74 kWh, 35.39 kVArh, 113.4 kW, and 85.17 kW, respectively.

Fig. 16 shows the active power generation of CHP facilities. As shown in Fig. 16, the CHPs were fully committed and the aggregated active power generation of these facilities was around 79.15 MWh.

Fig. 17 presents the aggregated power and reserve transactions of the aggregator with the ADSO. The net active and reactive power

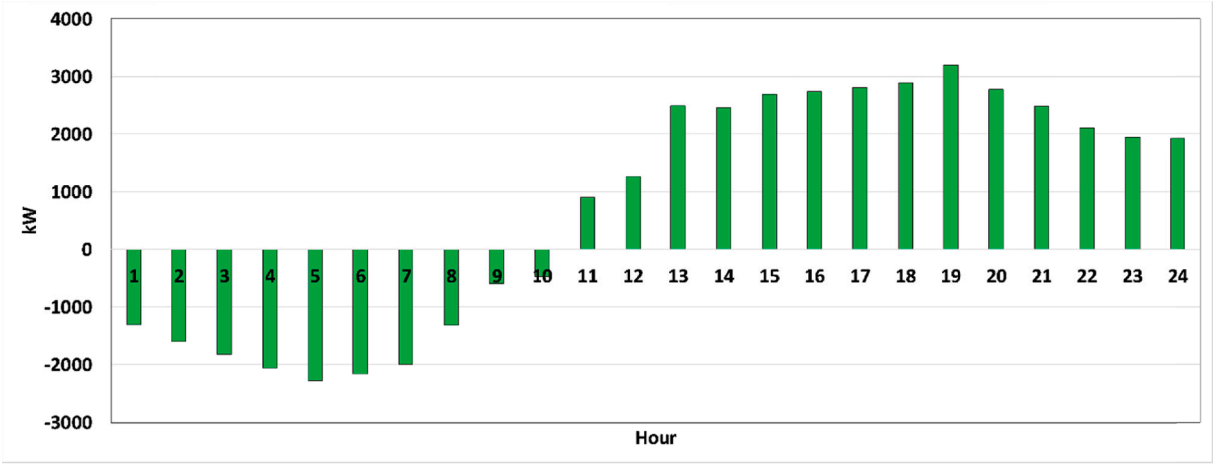

(a)

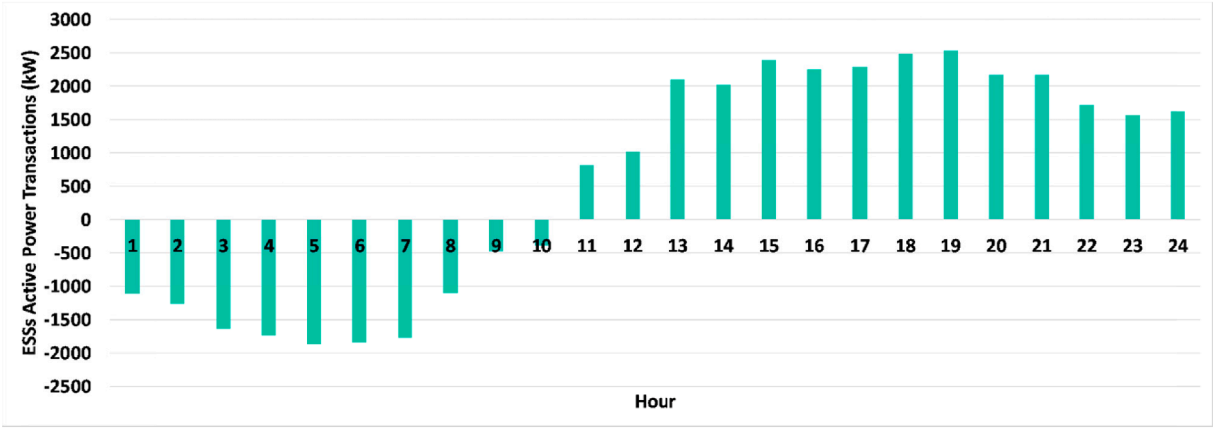

(b)

Fig. 14. (a) The accepted values of the active power of smart homes, (b) The energy transactions of ESSs.

transactions were around 107724.12 kWh and 65549.93 kVArh, respectively.

Fig. 18 depicts the aggregated cost/benefit of active power, reactive power, spinning reserve, and regulating reserve transactions of the aggregator with the ADSO. The net values of benefits of active and reactive power transactions were about 6.433 MMUs and 1,162,930 MUs, respectively. MU stands for the monetary unit. It was assumed that all of the ADSO bids were accepted by the upward market operator.

A sensitivity analysis was performed to assess the impacts of different values of active power and spinning reserve prices on the aggregators' benefits. Fig. 19 shows the aggregated cost/benefit of the aggregator for different values of active power and spinning reserve prices. The maximum values of the benefits of aggregators 1–6 were about 115,250 MUs, 75,761 MUs, 37,972 MUs, 55,936 MUs, 89,850 MUs, and 89,767 MUs, respectively. The maximum values of benefits of aggregators were decreased when the values of active power and spinning reserve prices were reduced.

Fig. 20 (a) and Fig. 20 (b) present the estimated values of the ADSO cost/benefit for active power, reactive power, spinning reserve, and regulating power transactions with the upward electricity market for different values of Γ.

Fig. 21 depicts the resiliency index for the corresponding worst-case external shocks that occurred without the proposed algorithm for the day-ahead optimization process. The resiliency indices tended to the infinity considering the proposed algorithm.

Fig. 22 (a) and (b) depict the real-time electrical load forecasting gaps for various forecasting periods.

Fig. 23 (a) shows the provided ramp of parking lots, DGs, and ESSs without considering the traffic patterns. Fig. 23 (b) shows the provided ramp of parking lots, DGs, and ESSs considering the traffic patterns. The aggregated provided ramp of parking lots without and considering the traffic patterns were about 126387.21 kWh and 52302.11 kWh, respectively. As shown in Fig. 23 (a), (b), the provided ramps of parking lots were decreased by about 58.61% based on the fact that the available ramp capacity of parking lots was reduced when the traffic patterns were encountered in the optimization process.

Fig. 24 depicts the benefit of the provided ramp of ADSO without and with the traffic patterns on routes. As shown in Fig. 24, the aggregated benefit of the provided ramp of ADSO without and with the traffic patterns on routes were 8.916 MMUs and 7.358 MMUs, respectively. The aggregated benefit of the provided ramp of ADSO was decreased by about 17.47% concerning the no-traffic case.

Fig. 25 presents the number of microgrid formations for the 64 worst-case external shocks for the real-time optimization process (15 min intervals). As shown in Fig. 25, the proposed optimization algorithm sectionalized the ADSO system into multi-microgrids to mitigate the impact of external shocks. The most credible external shock was named external shock 11 and occurred at 14:00 when lines 13–152 and 18–135

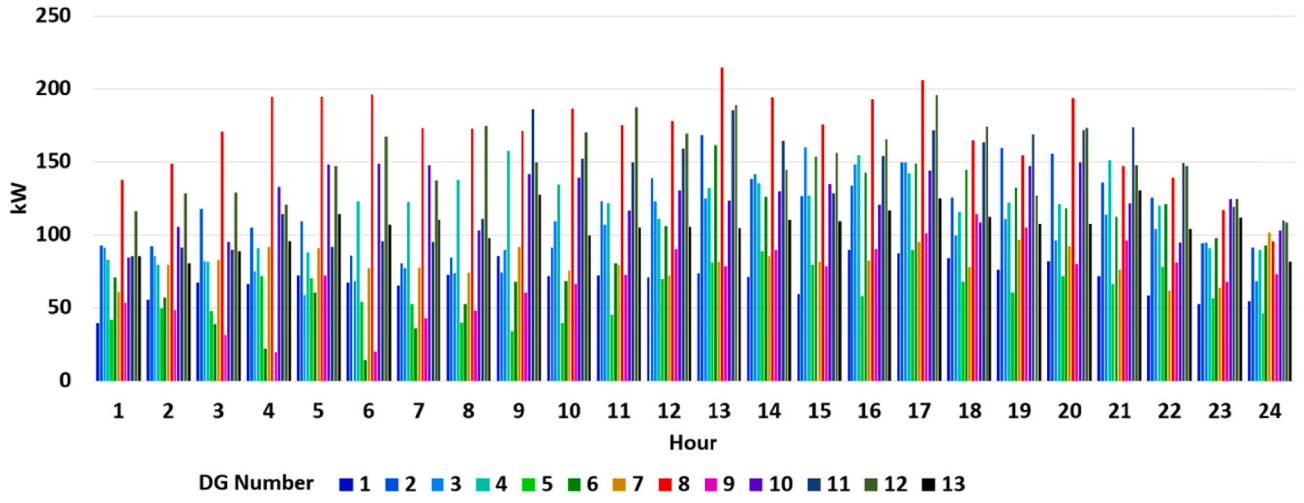

(a)

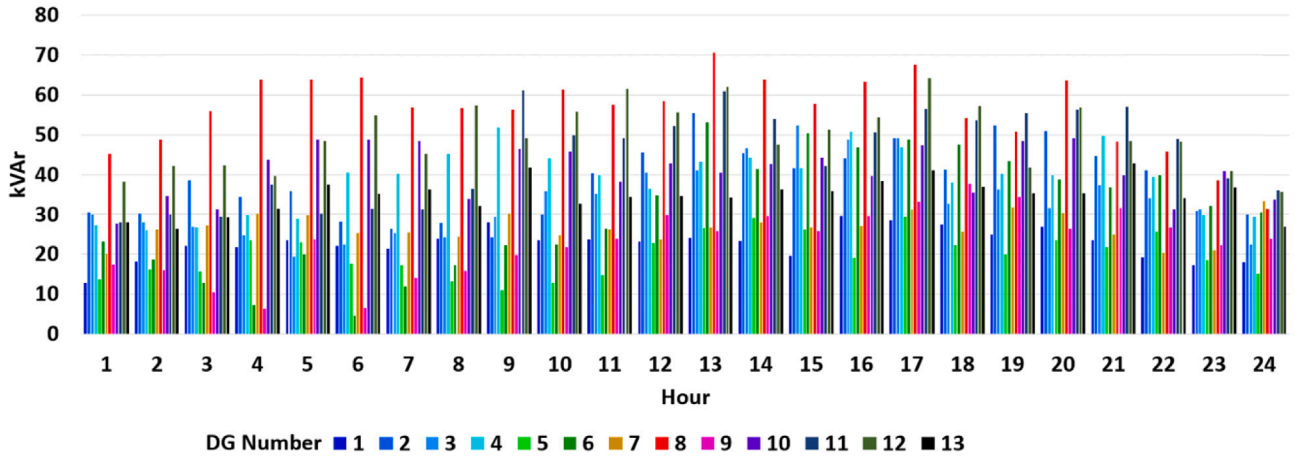

(b)

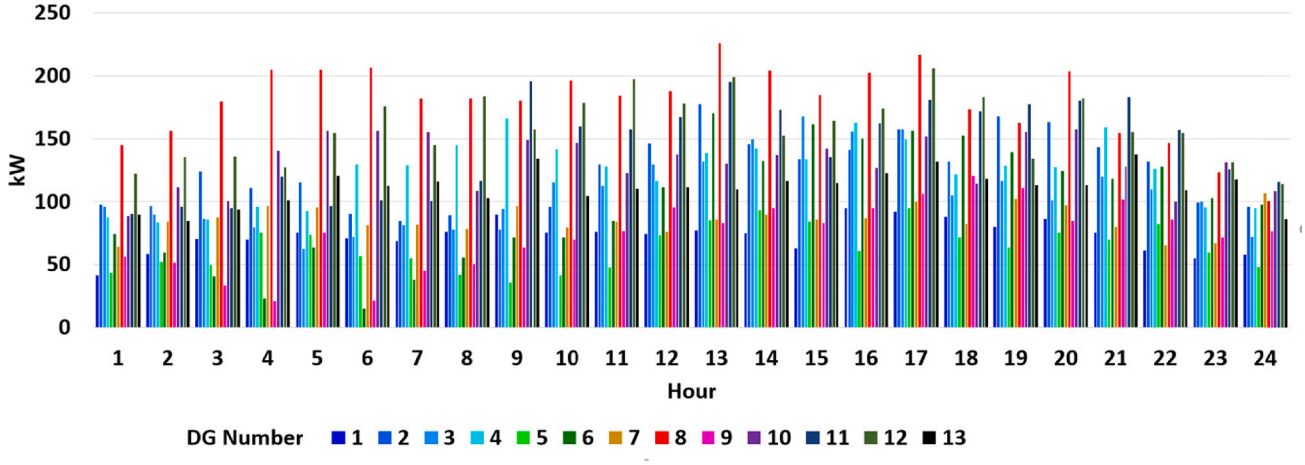

(c)

Fig. 15. (a) The accepted values of active power, (b) reactive power, (c) spinning reserve, (d) regulating reserve of distributed generation facilities for the day-ahead market.

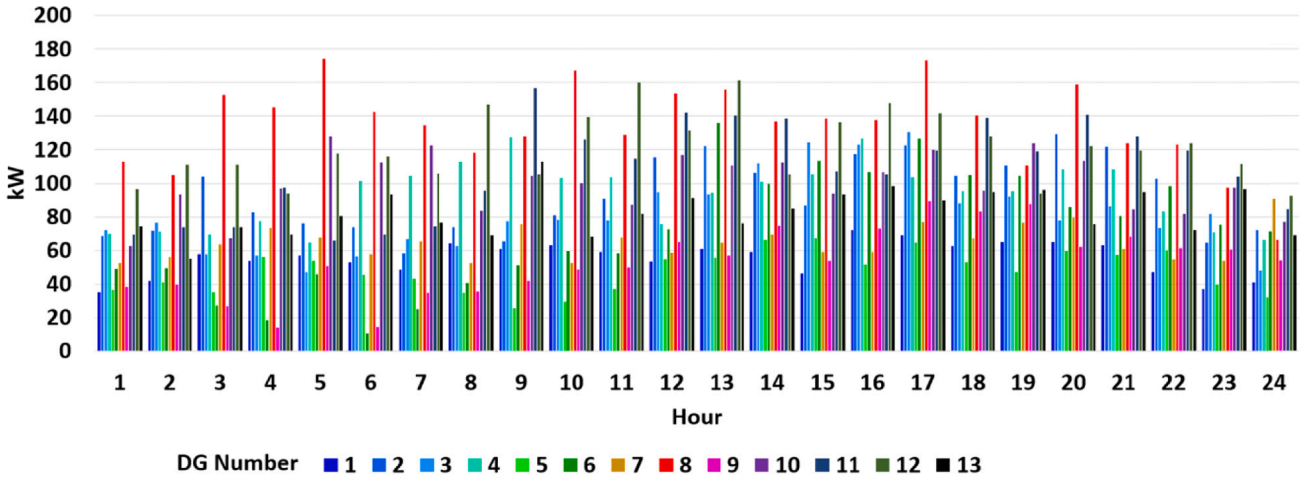

(d)

Fig. 15. (*continued*).

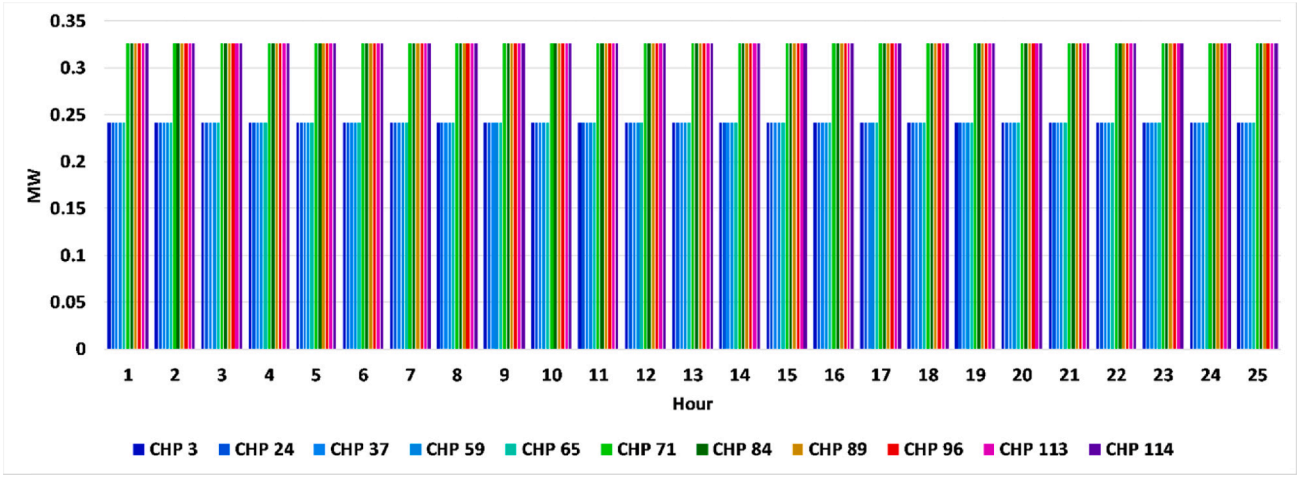

Fig. 16. The active power generation of CHP facilities for the day-ahead market.

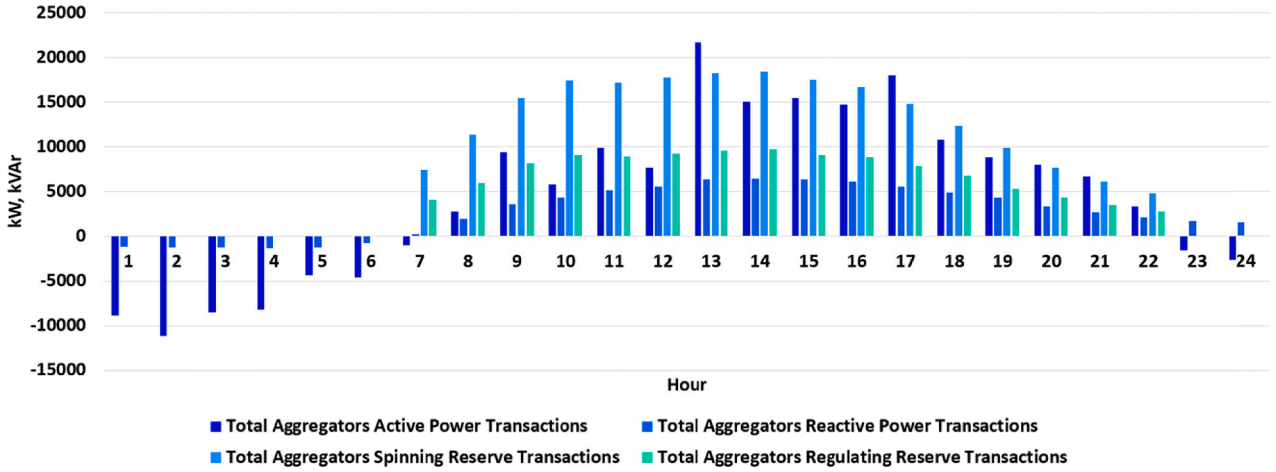

Fig. 17. The aggregated active power, reactive power, spinning reserve, and regulating reserve transactions of aggregator with the ADSO.

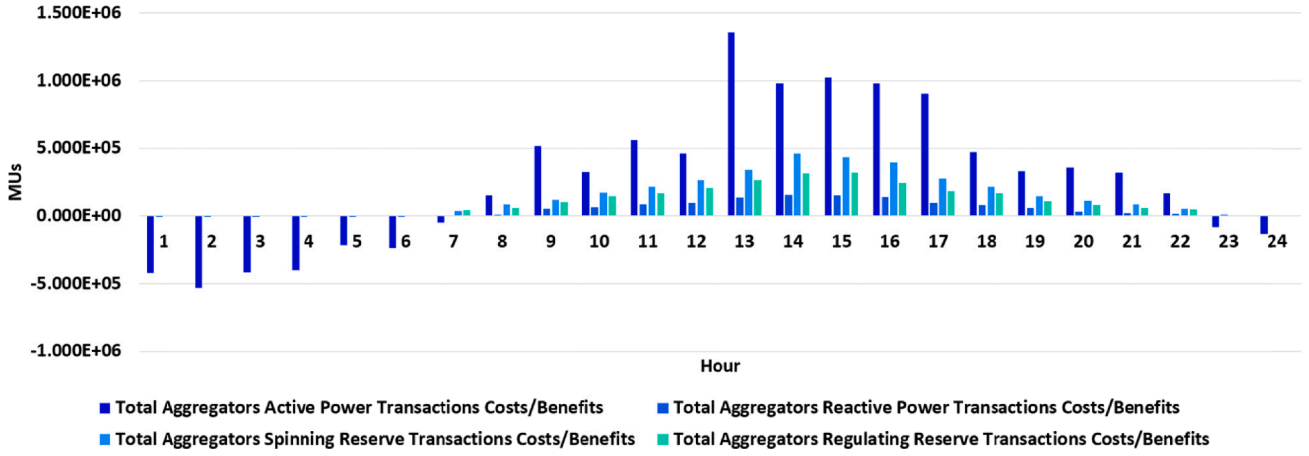

Fig. 18. The aggregated cost/benefit of active power, reactive power, spinning reserve, and regulating reserve transactions of aggregator with the ADSO.

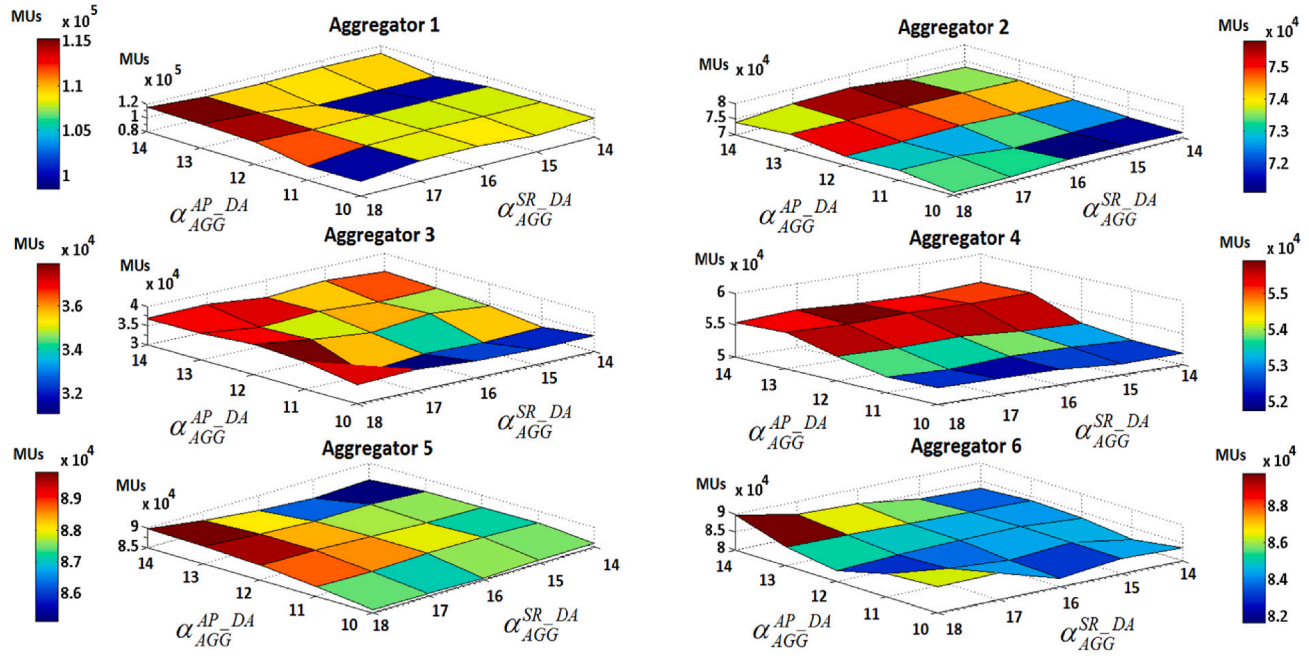

Fig. 19. The aggregated cost/benefit of the aggregator for different values of active power and spinning reserve prices.

were out of service. The 2nd, 3rd, 4th, 5th, and 6th zones were isolated from the upward system for the remained simulation interval. Thus, the optimization process sectionalized the system into the following two microgrids: 1) zone 1, 2) and zone 2–6.

Fig. 26 (a) and Fig. 26 (b) represent aggregated operating and interruption costs of ADSO for 64 worst-case external shocks without and with the proposed algorithm respectively.

Fig. 27 introduces the resiliency index for the corresponding worst-case external shocks that occurred without the proposed algorithm for the real-time optimization process. The resiliency indices for all of the considered external shocks tended to the infinity considering the proposed algorithm.

Fig. 28 (a) depicts the average values of real-time market active power and ancillary services prices of the upward market, and the average values of accepted active power and ancillary services prices of ADSO, aggregators, and parking lots. Further, Fig. 28 (b) provides the average values of real-time market active power and ancillary services prices of the upward market, the average values of accepted active power and ancillary services prices of ADSO, aggregators, and parking lots for the real-time optimization process for the worst-case external shock conditions that was occurred for 14:00.

Fig. 29 shows the active power generation of distributed generation facilities in normal and worst-case external shock conditions for the real-time process. The aggregated active power generations of distributed generation facilities for normal and worst-case external shock conditions were 135512.36 kWh and 160511.15 kWh, respectively. Thus, distributed generation units produced more energy by about 18.44% concerning the normal state of the system.

Fig. 30 presents the active power generation of smart homes in normal and worst-case external shock conditions for the real-time optimization process. The aggregated active power generations of smart homes for normal and worst-case external shock conditions were 65592.93 kWh and 80688.13 kWh, respectively. Thus, smart homes delivered more energy to the system by about 23.1% of the normal state of the system.

The simulation was carried out on a PC (AMD A10-5750 M processor, 4 × 2.5 GHz, 8 GB RAM). The max simulation time for the normal operational condition was around 9624 s, while for the worst-case contingent condition was around 1268 s.

Table 6 presents the variables and equations of the optimization

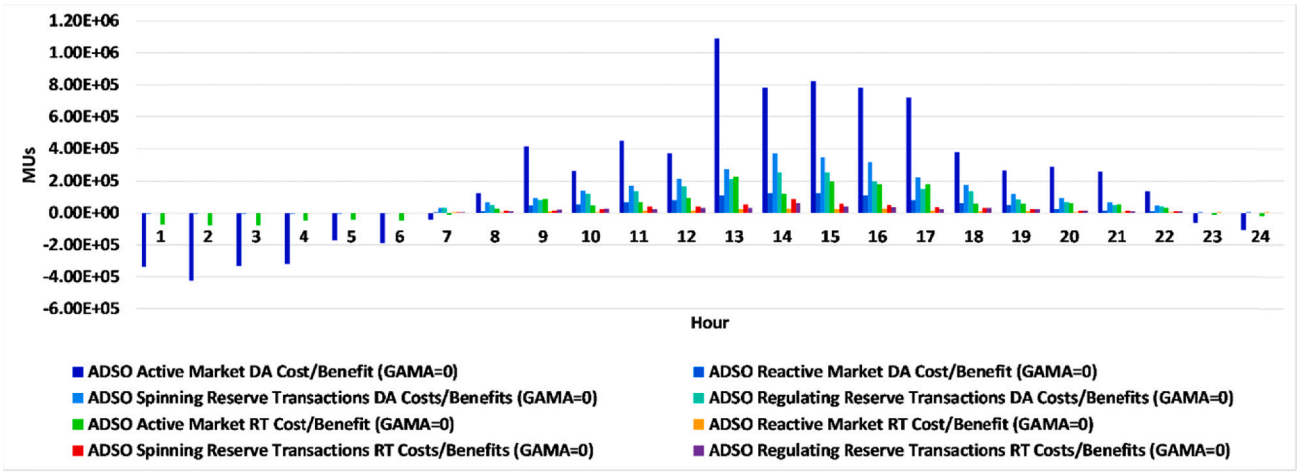

(a)

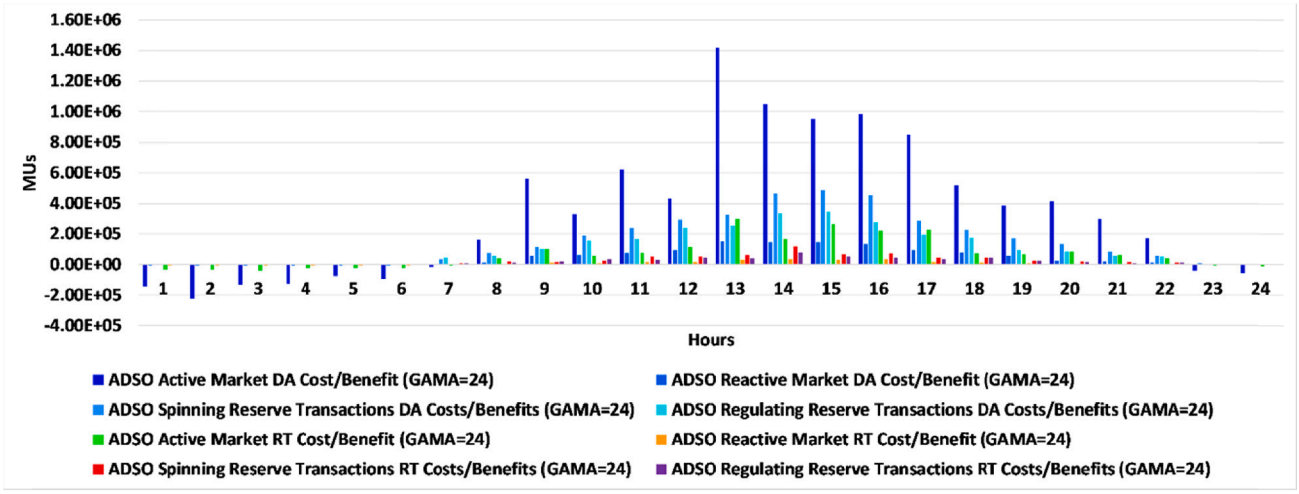

(b)

Fig. 20. (a) The estimated values of the ADSO cost/benefit for active power, reactive power, spinning reserve, and regulating power transactions with the upward electricity market for $\Gamma = 0$, (b) and for $\Gamma = 24$.

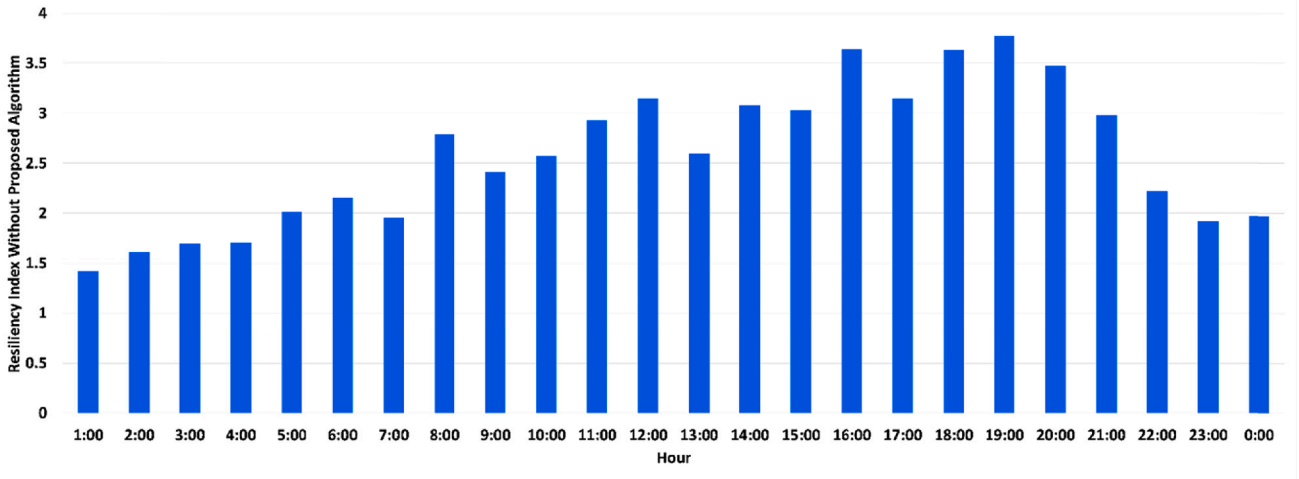

Fig. 21. The resiliency index for the corresponding worst-case external shocks that occurred without the proposed algorithm for the day-ahead optimization process.

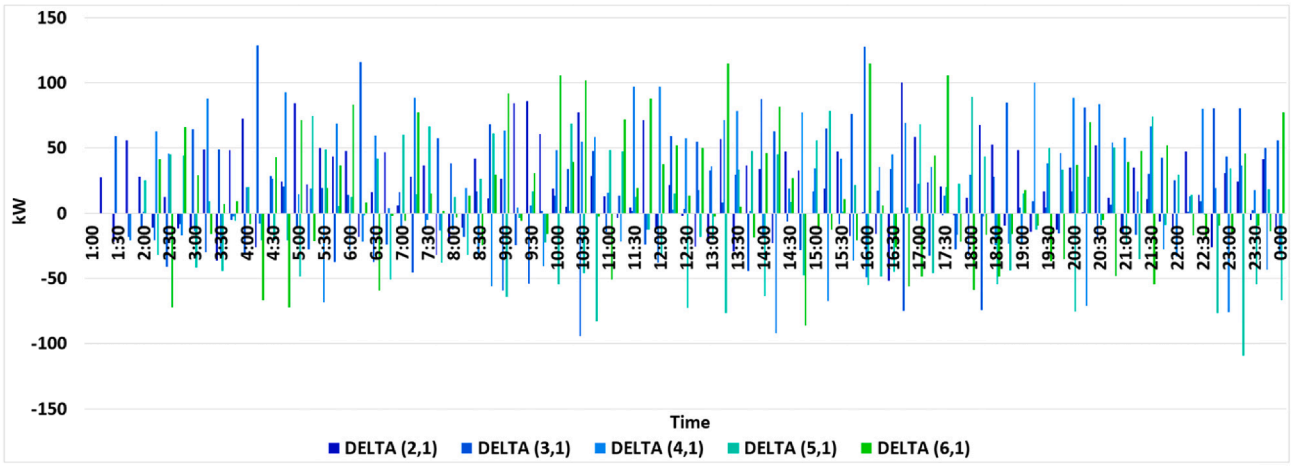

(a)

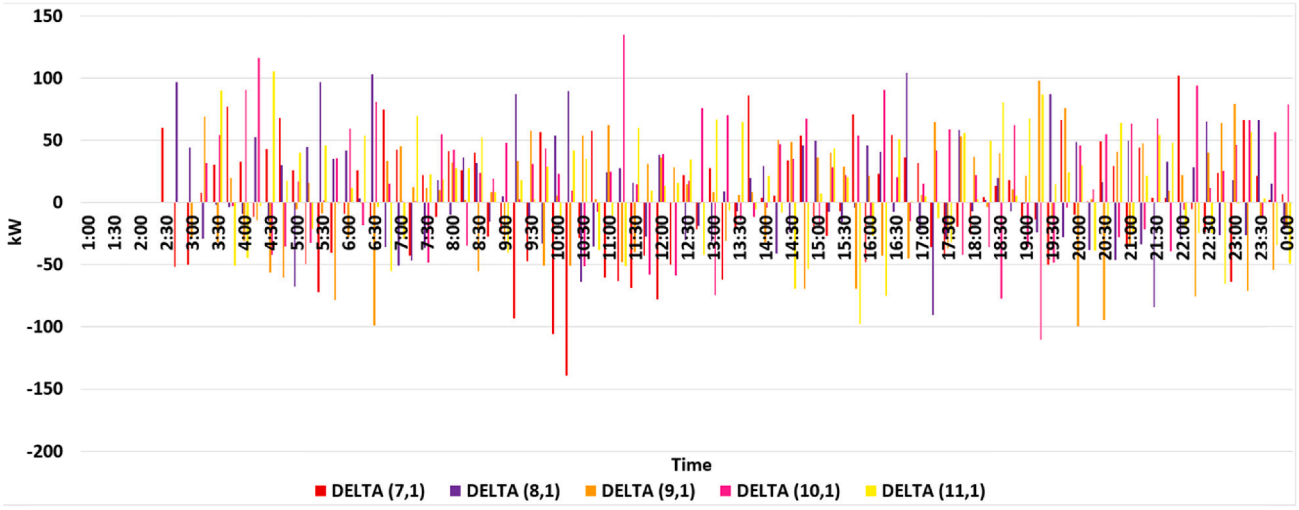

(b)

Fig. 22. (a) The real-time electrical load forecasting mismatches for the first-sixth 15 min real-time load forecasting process, (b) and for the seventh-eleventh 15 min.

model for various optimization levels.

In conclusion, the proposed method successfully determined the optimal scheduling of system resources and topology in the external shock conditions considering PHEVs commitment scenarios and traffic patterns of routes.

5. Conclusion

This paper introduced a two-stage model for the optimal resilient scheduling of an active distribution system in the day-ahead and real-time markets considering the traffic patterns and interactions of aggregators, parking lots, distributed energy resources, and plug-in hybrid electric vehicles. The first level maximized the plug-in hybrid electric vehicles for the day-head market considering estimated fuel consumption and traffic patterns on routes. The second level optimized the scheduling of parking lots and distributed energy resources. The third level maximized the aggregators' benefit in the day-ahead market. Finally, the fourth level maximized the benefit of the active distribution system in the day-ahead horizon considering the probable external shock of the system. The first, second, third, and fourth level problems of the second-stage optimization process optimized the plug-in electric vehicles, parking lots, and distributed energy resources, aggregators, and distribution system in the real-time market. The traffic of routes reduced the ramp-up and ramp-down transactions of the distribution system by about 58.61%. Further, the aggregated benefit of the provided ramp was decreased by about 17.47% concerning the no-traffic case. The proposed approach decreased the aggregated operating and interruption costs of ADSO by around 94.56% concerning the 64 worst-case external shock conditions. Finally, the smart homes injected more energy into the system in external shock conditions by about 23.1% concerning the normal state of the system. The authors are working on the modeling of mobile energy storage facilities commitments in external shock conditions for consideration in the proposed algorithm.

CRediT authorship contribution statement

Mehdi Firouzi: Investigation, Data curation, Writing – original draft. **Mehrdad Setayesh Nazar:** Conceptualization, Methodology,

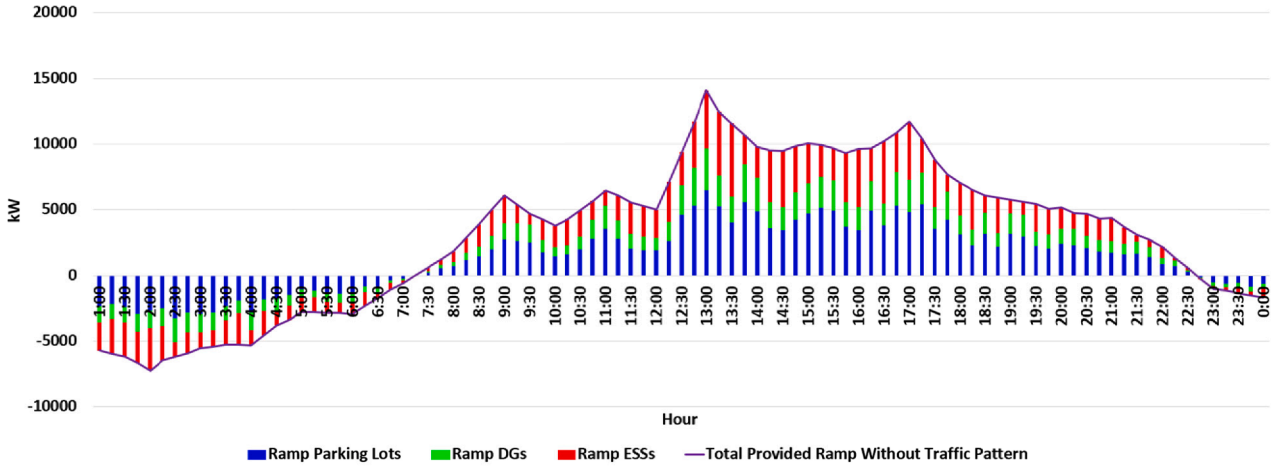

(a)

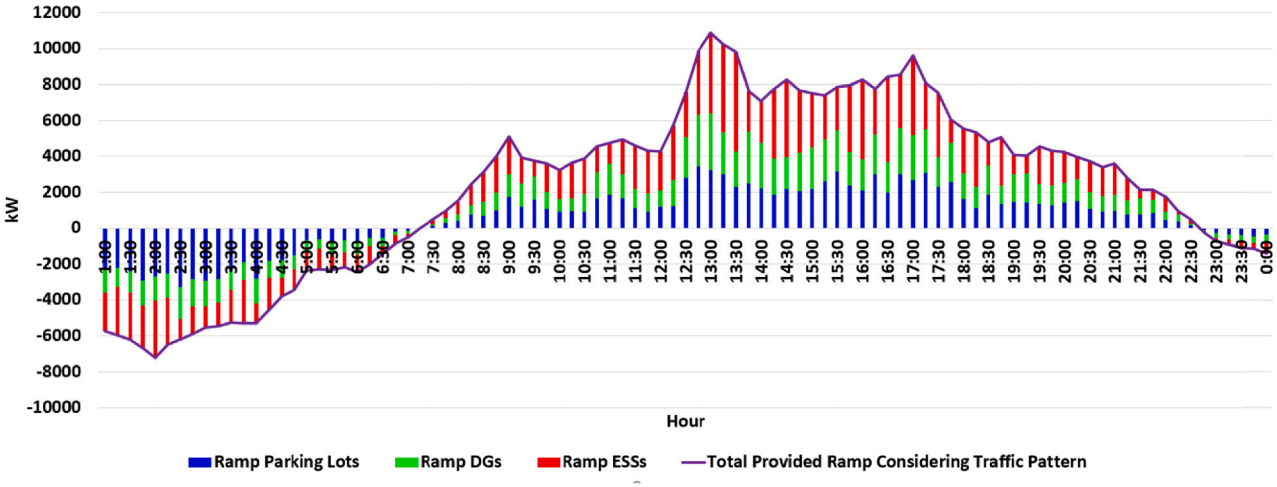

(b)

Fig. 23. (a) The provided ramp of parking lots, DGs, and ESSs without considering the traffic patterns on routes, (b) and considering the traffic patterns on routes.

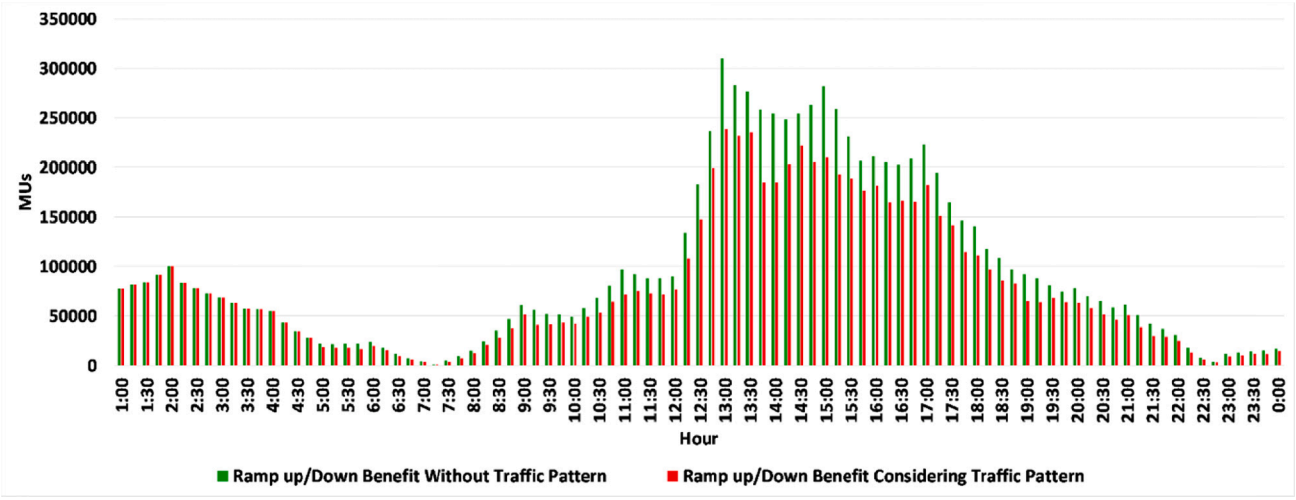

Fig. 24. The benefit of the provided ramp of ADSO without and with the traffic patterns on routes.

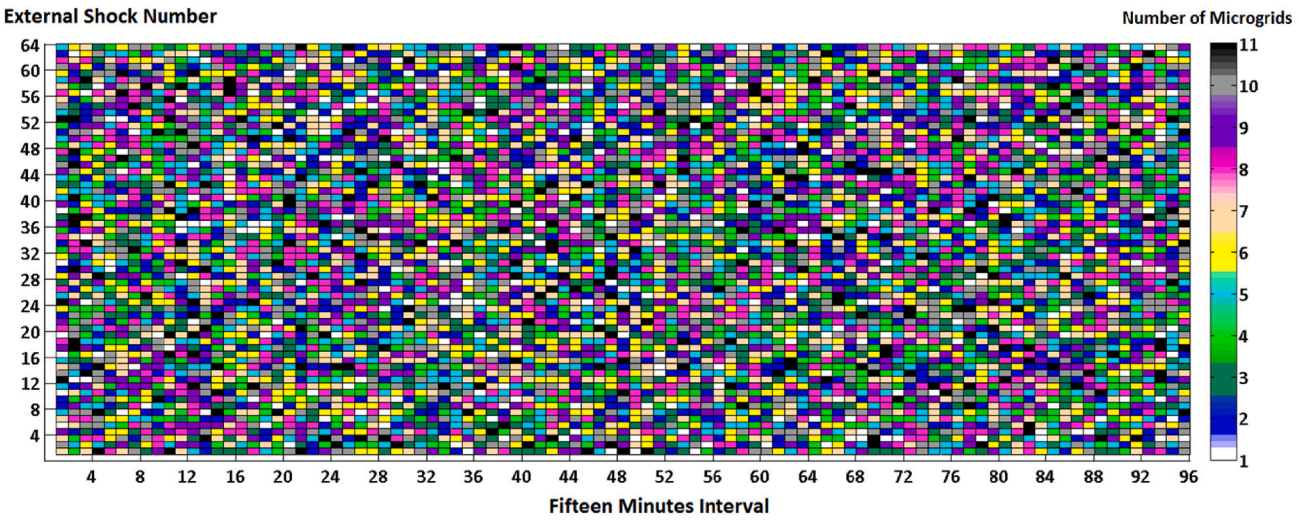

Fig. 25. The number of microgrid formations for the 64 worst-case external shocks.

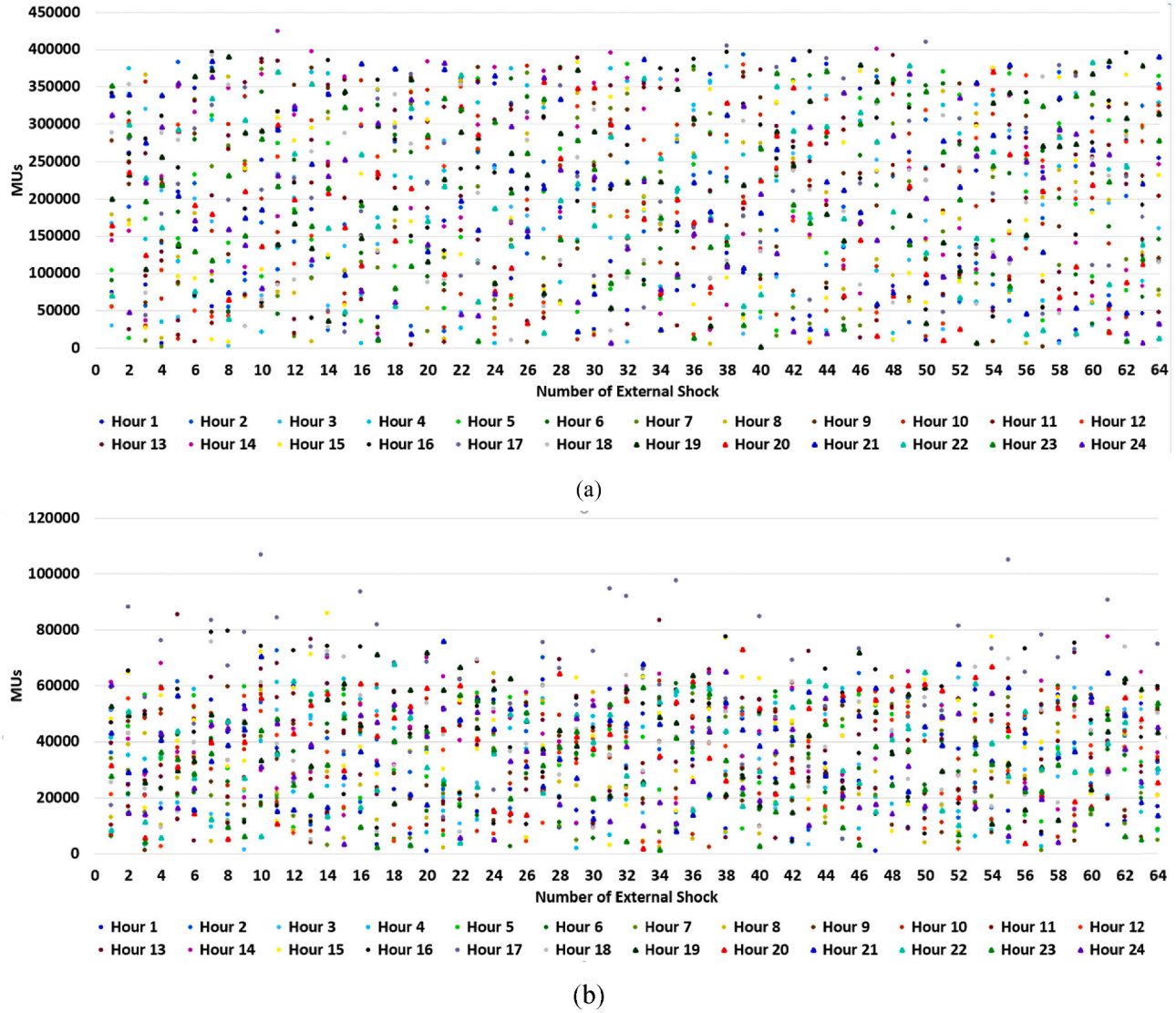

Fig. 26. The aggregated operating and interruption costs of ADSO for the 64 worst-case external shocks without (a) and with (b) the proposed algorithm for the real-time optimization process.

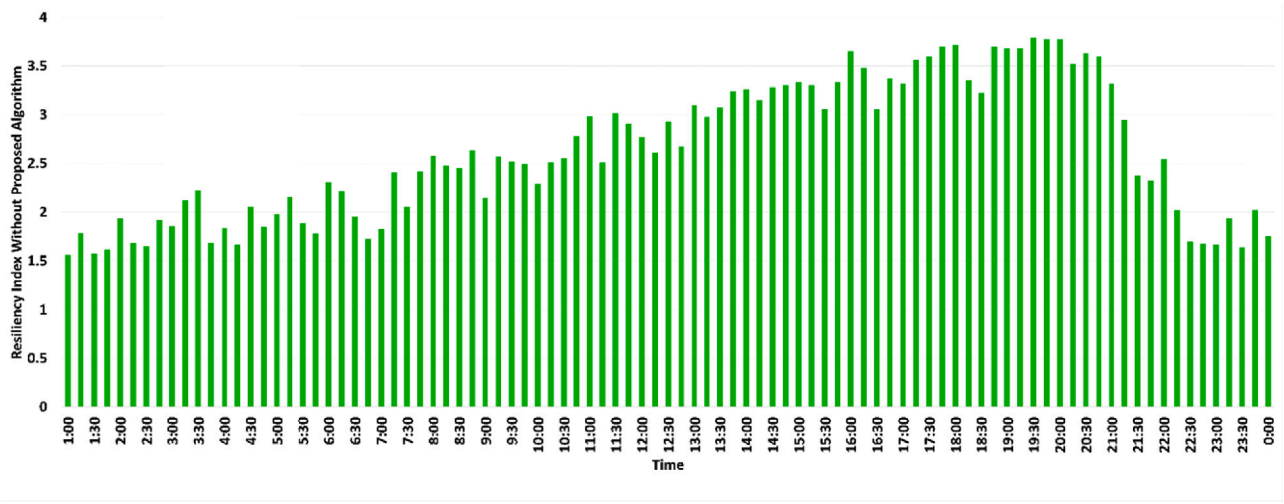

Fig. 27. The resiliency index for the corresponding worst-case external shocks that occurred without the proposed algorithm for the real-time optimization process.

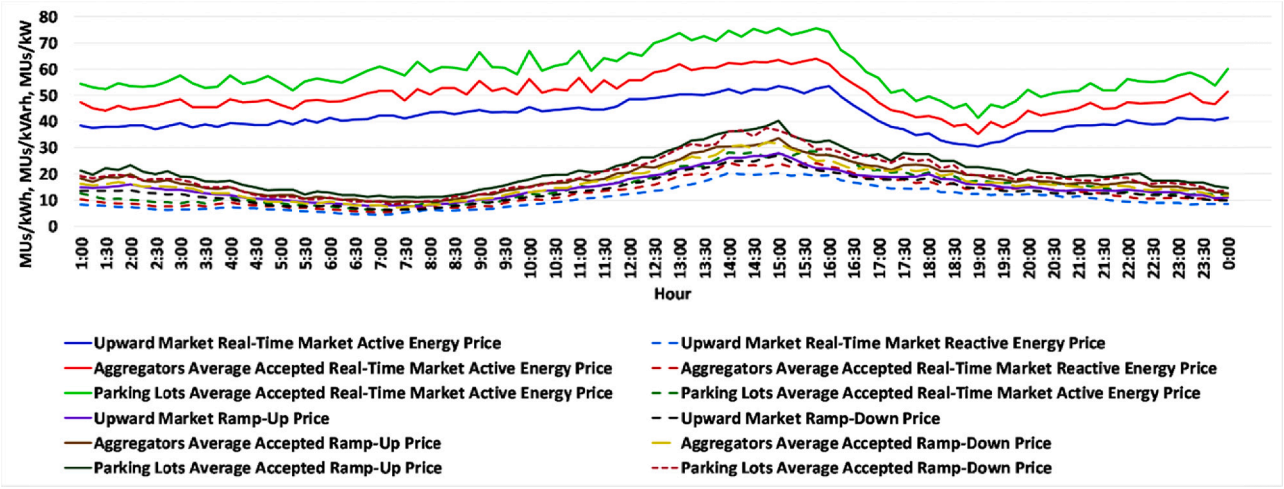

(a)

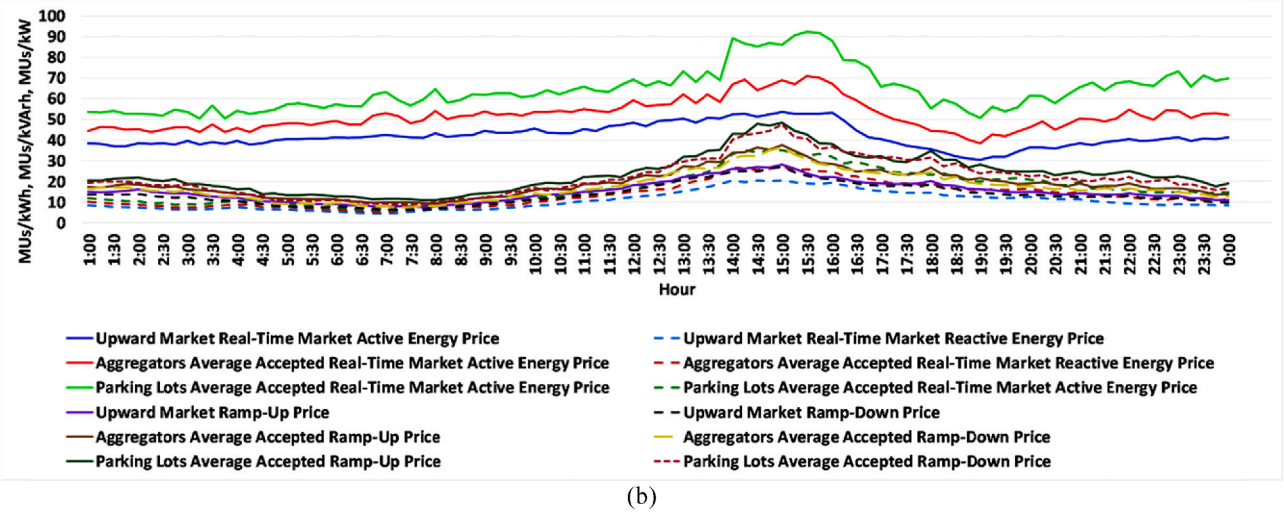

(b)

Fig. 28. (a) The average values of real-time market active power and ancillary services prices of the upward market, ADSO, aggregators, and parking lots for the real-time optimization process in normal operating conditions, (b) and for the worst-case external shock conditions.

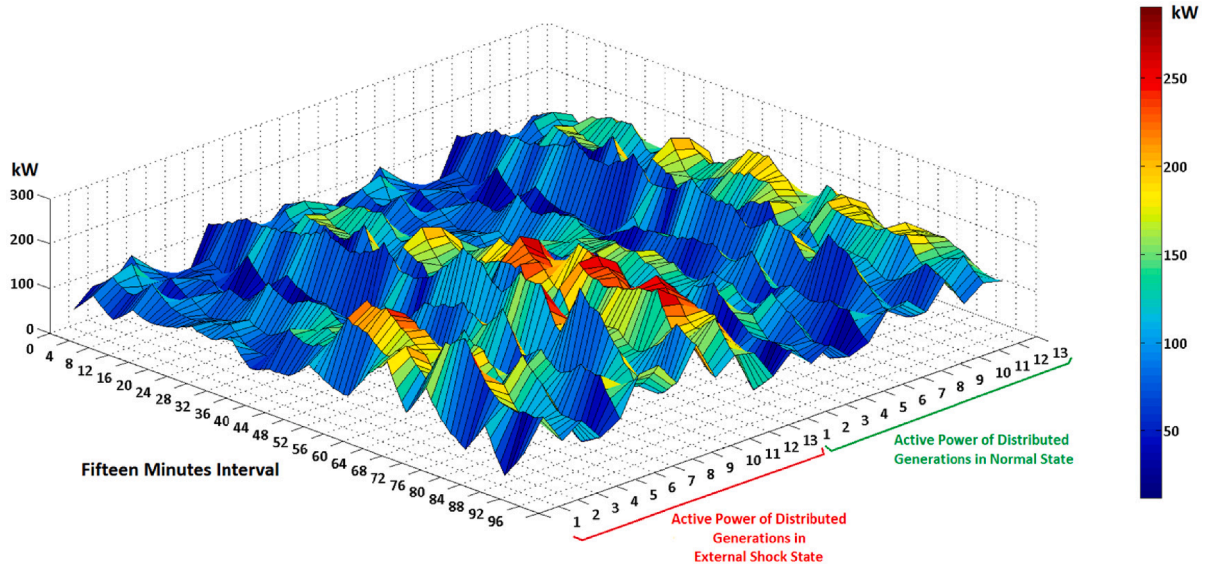

Fig. 29. The active power generation of distributed generation facilities in normal and worst-case external shock conditions for the real-time optimization process.

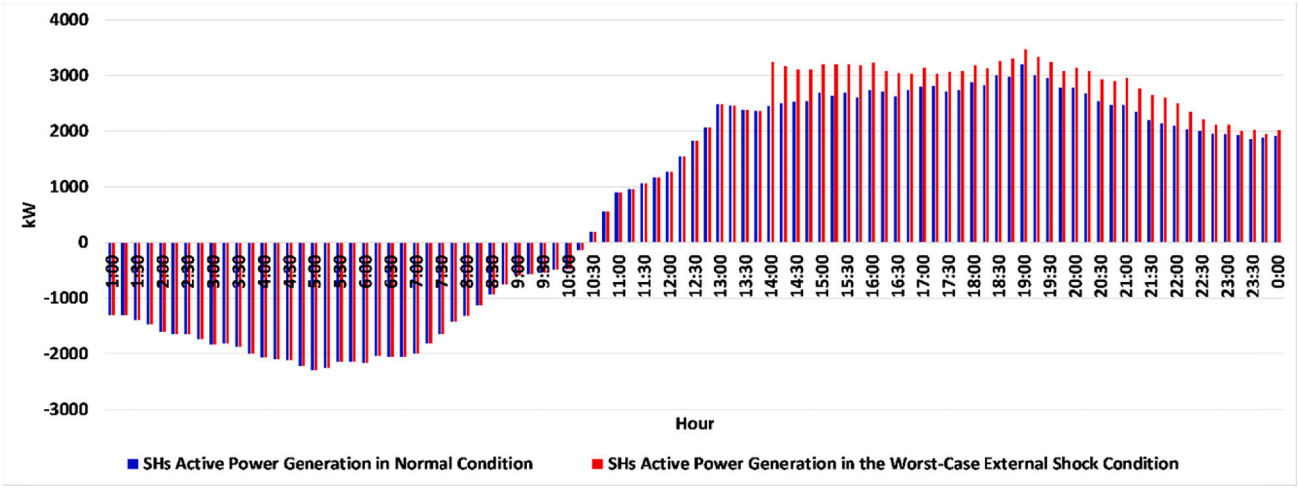

Fig. 30. The active power generation of smart homes in normal and worst-case external shock conditions for the real-time optimization process.

Table 6
Variables and equations of the optimization model for various optimization levels.

Operation Mode	Level of optimization	CPU time (sec)	Cont. variables	Disc. variables
Day-ahead optimization process	1	1729	1,129,624	524
	2	3824	1,423,915	986
	3	6514	1,632,628	1024
	4	9624	1,769,621	1232
Real-time optimization process	1	115.2	162,036	3268
	2	136.1	181,536	3644
	3	149.0	259,335	3812
	4	211.2	286,328	4124

Supervision. **Miadreza Shafie-khah:** Formal analysis, Validation. **João P.S. Catalão:** Visualization, Writing – review & editing.

Declaration of Competing Interest

The authors declare that they have no known competing financial interests or personal relationships that could have appeared to influence the work reported in this paper.

Data availability

The data that has been used is confidential.

References

[1] Aboutalebi M, Setayesh Nazar M, Shafie-khah M, Catalão JPS. Optimal scheduling of self-healing distribution systems considering distributed energy resource capacity withholding strategies. Int J Electr Power Energy Syst 2022;136:107662.

[2] Nourollahi R, Salayani P, Zare K, Mohammadi Ivatloo B. Resiliency-oriented optimal scheduling of microgrids the presence of demand response programs using a hybrid stochastic robust optimization approach. Int J Electr Power Energy Syst 2021;128:106723.

[3] Hosseinnia H, Modarresi J, Nazarpour D. Optimal eco-emission scheduling of distribution network operator and distributed generator owner under employing demand response program. Energy 2020;191:116553.

[4] Fotouhi Ghazvini MA, Soares J, Abrishambaf O, Castro R, Vale Z. Demand response implementation in smart households. Energy Build 2017;143:129-148.

[5] Xu NZ, Chung CY. Reliability evaluation of distribution systems including vehicle-to-home and vehicle-to-grid. IEEE Trans. on Power Systems 2015;31:759–68.

[6] Gholami A, Shekari T, Aminifar F, Shahidehpour M. Microgrid scheduling with uncertainty: the quest for resilience. IEEE Trans Smart Grid 2016;7:2849–58.

[7] Rahimi K, Davoudi M. Electric vehicles for improving resilience of distribution systems. Sustain Cities Soc 2018;36:246–56.

[8] Bagheri Tookanlou M, Pourmousavi Kani SA, Marzband M. A comprehensive day-ahead scheduling strategy for electric vehicles operation. Int J Electr Power Energy Syst 2021;131:106912.

[9] Zhang Z, He H, Guo J, Han R. Velocity prediction and profile optimization based real-time energy management strategy for Plug-in hybrid electric buses. Appl Energy 2020;280:116001.

[10] Kaur K, Singh M, Kumar N. Multiobjective optimization for frequency support using electric vehicles: an aggregator-based hierarchical control mechanism. IEEE Syst J 2019;13:771–82.

[11] Lei Z, Qin D, Zhao P, Li J, Liu Y, Chen Z. A real-time blended energy management strategy of plug-in hybrid electric vehicles considering driving conditions. J Cleaner Product 2020;252:119735.

[12] Heydarian-Forushani E, Golshan MEH, Shafie-khah M, Siano P. Optimal operation of emerging flexible resources considering sub-hourly flexible ramp product. IEEE Trans Sustain Energy 2018;9:916–29.

[13] Wu Y, Tan H, Peng J, Zhang H, He H. Deep reinforcement learning of energy management with continuous control strategy and traffic information for a series-parallel plug-in hybrid electric bus. Appl Energy 2019;247:454–66.

[14] Neyestani N, Damavandi MY, Shafie-khah M, Bakirtzis AG, Catalão JPS. Plug-in electric vehicles parking lot equilibria with energy and reserve markets. IEEE Trans Power Syst 2017;32:2001–16.

[15] Montazeri-Gh M, Mahmoodi-K M. Optimized predictive energy management of plug-in hybrid electric vehicle based on traffic condition. J Clean Product 2016; 139:935–48.

[16] Zolfaghari Moghaddam S, Akbari T. Network-constrained optimal bidding strategy of a plug-in electric vehicle aggregator: a stochastic/robust game theoretic approach. Energy 2018;151:478–89.

[17] Zhang B, Kezunovic M. Impact on power system flexibility by electric vehicle participation in ramp market. IEEE Trans Smart Grid 2016;7:1285–94.

[18] Guo Z, Li G, Zhou M, Feng W. Resilient configuration approach of integrated community energy system considering integrated demand response under uncertainty. 2019. IEEE Access 7, pp. 87513–87533.

[19] H. Mehrjerdi, R. Hemmati, Coordination of vehicle-to-home and renewable capacity resources for energy management in resilience and self-healing building" 2020. Renew Energy 2020;146:568-579.

[20] Eseye A, Lehtonen M, Tukia T, Uimonen S, Millar R. Optimal energy trading for renewable energy integrated building microgrids containing electric vehicles and energy storage batteries. IEEE Access 2019;7:106092–101.

[21] Hafiz F, Chen B, Chen C, de Queiroz AR, Husain I. Utilising demand response for distribution service restoration to achieve grid resiliency against natural disasters", 2019. IET Gener Transm Distrib 2019;13:2942-2950.

[22] Hussain A, Bui VH, Kim HM. A resilient and privacy-preserving energy management strategy for networked microgrids. IEEE Trans Smart Grid 2016;9: 2127–39.

[23] Hussain A, Bui VH, Kim HM. Microgrids as a resilience resource and strategies used by microgrids for enhancing resilience. Appl Energy 2019;240:56–72.

[24] Wang Z, Wang J. Self-healing resilient distribution systems based on sectionalization into microgrids. IEEE Trans Power Syst 2015;30:3139–49.

[25] Zhu J, Yuan Y, Wang W. An exact microgrid formation model for load restoration in resilient distribution system. Int J Electr Power Energy Syst 2020;116:105568.

[26] Farzin H, Fotuhi-Firuzabad M, Moeini-Aghtaie M. Enhancing power system resilience through hierarchical outage management in multi-microgrids. IEEE Trans Smart Grid 2016;7:2869–79.

[27] Guo Z, Li G, Zhou M, Feng W. Resilient configuration approach of integrated community energy system considering integrated demand response under uncertainty. 2019, IEEE Access, 7, 87513–87533.

[28] Khalili T, Tarafdar Hagh M, Gassem Zadeh S, Maleki S. Optimal reliable and resilient construction of dynamic self-adequate multi-microgrids under large-scale events. IET Generat Transm Distribut 2019;10:1750–60.

[29] Arefifar SA, Mohamed YA, El-Fouly TH. Comprehensive operational planning framework for self-healing control actions in smart distribution grids. IEEE Trans Power Syst 2013;28:4192–200.

[30] Chanda S, Srivastava AK. Defining and enabling resiliency of electric distribution systems with multiple microgrids. IEEE Trans Smart Grid 2016;7:2859–68.

[31] Zakernezhad H, Setayesh Nazar M, Shafie-khah M, Catalão JPS. Optimal scheduling of an active distribution system considering distributed energy resources, demand response aggregators and electrical energy storage. Appl Energy 2022;314:118865.

[32] Lin C, Chen C, Liu F, Li G, Bie Z. Dynamic MGs-based load restoration for resilient urban power distribution systems considering intermittent RESs and droop control. Int J Electr Power Energy Syst 2020;140:107975.

[33] Wu C, Chen C, Ma Y, Li F, Sui Q, Lin X, et al. Enhancing resilient restoration of distribution systems utilizing electric vehicles and supporting incentive mechanism. Appl Energy 2022;322:119452.

[34] Diahovchenko M, Kandaperumal G, Srivastava AK, Maslova ZI, Lebedka SM. Resiliency-driven strategies for power distribution system development. Electric Power Systems Res 2021;197:107327.

[35] Silva JAA, López JC, Arias NB, Rider MJ, da Silva LCP. An optimal stochastic energy management system for resilient microgrids. Appl Energy 2021;300: 117435.

[36] Zakernezhad H, Setayesh Nazar M, Shafie-khah MR, Catalão JPS. Optimal resilient operation of multi-carrier energy systems in electricity markets considering distributed energy resource aggregators. Appl Energy 2021;299:117271.

[37] Liu J, Lin G, Huang S, Zhou Y, Rehtanz C, Li Y. Collaborative EV routing and charging scheduling with power distribution and traffic networks interaction. IEEE Trans Power Syst 2022;37:3923–36.

[38] Luo Y, Zhu T, Wan S, Zhang S, Li K. Optimal charging scheduling for large-scale EV (electric vehicle) deployment based on the interaction of the smart-grid and intelligent-transport systems. Energy 2016;97:359–68.

[39] Eichhorn A, Heitsch H, W. Römisch. Stochastic optimization of electricity portfolios: Scenario tree modeling and risk management. Berlin, Heidelberg: Springer; 2010.

[40] Heitsch H, W. Römisch. Scenario reduction algorithms in stochastic programming. Computat Optim Appl 2003;24:187–206.

[41] Bostan A, Setayesh Nazar M, Shafie-khah MR, Catalão JPS. An integrated optimization framework for combined heat and power units, distributed generation and plug-in electric vehicles. Energy 2020;202:117789.